EXECUTIVE SUMMARY

Voyager continues an unparalleled mission of discovery, exploring the outer heliosphere in a journey to the edge of interstellar space and beyond. Voyager 1 (V1) is close to the termination shock (TS) of the supersonic solar wind. When V1 reaches the TS, we will know its strength, observe the shock acceleration of anomalous cosmic rays (ACRs), and study the effects of a shock that is several orders of magnitude larger in scale than any previously observed in situ. Beyond the TS we will explore an entirely new region, the heliosheath, and determine its structure, radial and temporal evolution, and the effects of changes in the solar wind on the hot, subsonic flow. The ultimate goal is to cross the heliopause into interstellar space and make the first *in situ* measurements of the local interstellar medium (LISM).

The two Voyager spacecraft provide information on radial, latitudinal, and temporal solar wind structure as they head for the TS, heliosheath, heliopause, and finally the LISM. Evidence of the solar wind interaction with the neutral component of the LISM is clear, with the speed at Voyager 2 (V2) down by 12-14% compared to that at 1 AU and the temperature increasing. Additional evidence of the approach to the shock comes from the first detection of cosmic ray electrons by V1. V1, at 85 AU, recently discovered intense outward flowing beams of keV to MeV particles. During this event, which has lasted at least 6 months, particle intensities increased by over an order of magnitude. The source of this event, which is not observed at V2, is not known.

Recent work shows that most (80-90%) of the cosmic ray modulation occurs outside the TS. Observations of heliosheath structure will help us understand the cause of the modulation. Voyager has just received the initial heliospheric radio emission from this solar cycle; despite numerous attempts to predict when this would occur, none succeeded, emphasizing the need for more data. Theory predicts that the heliosheath will be a very dynamic region; again, understanding the structures which form as the solar wind propagates through the heliosheath is crucial.

Future work encompasses several tasks. Inside the TS, we will study solar wind evolution and interaction with the LISM. At the next solar minimum, V2 will be at a high enough latitude to monitor the interaction region between the fast and slow wind and to observed coronal hole flow at large distances. We will continue to monitor and try to understand the outward flowing particles detected at large intensities by V1, as well as those observed at lower intensities by V2. We will observe the recovery of cosmic rays beyond 100 AU at solar minimum, determine the effects of a negative magnetic polarity solar cycle, monitor the unfolding of the low energy ACR spectra as V1 approaches the TS, and search for additional bursts of heliospheric radio emission. V1 will likely be in the vicinity of the TS for much of the next four years before it durably enters the heliosheath and begins the next phase of its journey to the edge of interstellar space.

1. INTRODUCTION

The Voyager Interstellar Mission is a three-phase mission. We are currently in the first phase, the study of the evolution and structure of the supersonic solar wind and associated waves and energetic particles in the outer heliosphere and their interaction with the neutral component of the LISM. The Voyager spacecraft have documented the transformation of the supersonic solar wind from a regime dominated by corotating streams which form corotating interaction regions (CIRs), to a regime where CIRs have coalesced into merged CIRs (CMIRs), to the current regime where corotating structure is lost and the structure is dominated by merged interaction regions (MIRs) with time scales of several solar rotations. Concurrently, pickup ions formed from ionization of the interstellar neutrals increased in importance and they now provide most of the internal pressure of the solar wind. Voyager is able to document these changes as a function of distance and solar cycle, as well as to investigate structure which may occur upstream of the TS. This phase of the mission will culminate with the first crossings of the TS, the boundary at which the solar wind becomes subsonic and is deflected as it begins the velocity change necessary to flow down the heliotail. This shock is thought to be a prodigious particle accelerator and the generation region of the ACRs.

The second phase will be the exploration of another entirely new region, the heliosheath. This region of subsonic flow should be active, containing both structures entrained in the solar wind and those generated by the motions of the TS. Only recently was the role of this region in the modulation of the galactic cosmic rays (GCRs) recognized [*McDonald et al.*, 2002]. The heliosheath phase will end and the third phase begin with the crossings of the heliopause, the discontinuity between the solar and interstellar plasma, and the achievement of the Voyager's ultimate goal: The first *in situ* measurements of the interstellar medium. We stress that in all of three phases the Voyagers will explore new regions and the promise of true discovery is high. For example, in July 2002 V1 entered an unexpected, and as yet poorly understood, region containing high intensities of very anisotropic particles with keV to MeV energies. These and other recent data are described in the science sections.

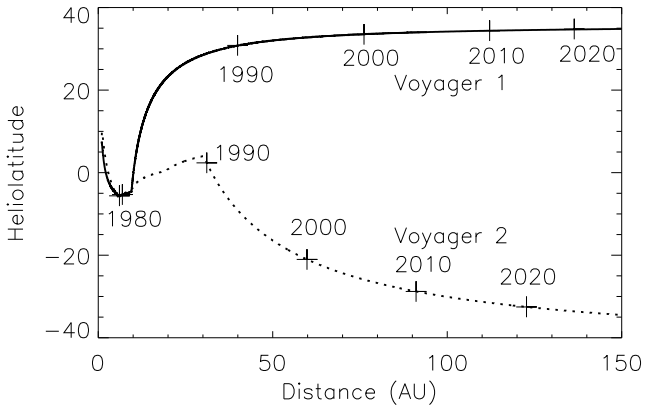

FIGURE 1. Trajectories of the Voyager spacecraft.

Figure 1 shows V1 and V2 distances and heliolatitudes as a function of time. V1 is at mid-northern latitudes and beyond 85 AU. V2 is at mid-southern latitudes and beyond 70 AU. A major advantage of the Voyager mission is that the outward speed is relatively slow, 3.1-3.6 AU/year, enabling us to observe solar-cycle variations as well as radial structure. The presence of two spacecraft, both headed roughly toward the nose of the heliosphere, allows some separation of radial from temporal and latitudinal structure.

The Voyager mission is directly relevant, and indeed essential, to the Sun Earth-Connection (SEC) science objectives. One primary Sun-Earth Connection science objective is to "Understand the changing flow of energy and matter throughout the Sun, heliosphere, and planetary environments". A focus area under this objective is to "Determine the evolution of the heliosphere and its interaction with the galaxy". Voyager provides the only new *in situ* measurements beyond 10 AU and provides crucial data for understanding how the heliosphere evolves and interacts with the galaxy via the local interstellar medium. A second prime objective is to "Explore the fundamental physical processes of plasma systems in the solar system", with a focus area to "Understand coupling across multiple scale lengths and its generality in plasma systems". Voyager provides information on length scales from gyroradii to tens of AU. For example, the coupling of the solar wind regime with the LISM neutrals occurs over many tens of AU, but results from pickup-ion acceleration which occurs within a gyroperiod. A third prime objective is to "Learn how galaxies, stars, and planets form, interact, and evolve" with research focus areas "delineate the current state of the local interstellar medium and its implications for galactic evolution" and "determine the interaction between the interstellar medium and the astrospheres of the Sun and other stars." Voyager is now indirectly sampling the LISM via its effects on the solar wind and has a good chance of making *in situ* LISM measurements. Another research focus area to which Voyager will contribute is to "develop the capability to predict solar activity and the evolution of solar disturbances as they propagate in the heliosphere and affect the Earth". A focus of recent Voyager work has been tracing events (shocks and CME ejecta) from the Sun to Earth to the outer heliosphere. The Voyager spacecraft will contribute significantly to the outstanding research issues identified by the SEC road map; for many of the objectives listed above, Voyager is uniquely able to do so.

The Voyager spacecraft and instruments are generally in good health. The instrument teams still active are the Plasma Science experiment (PLS) which measures thermal plasma, the Low Energy Charged Particle experiment (LECP) which detects particles in the tens of keV to tens of MeV range, the Cosmic Ray subsystem (CRS) which measures galactic and anomalous cosmic rays, the magnetometer experiment (MAG), and the Plasma Wave subsystem (PWS) which observes plasma and radio waves. In addition, the Planetary Radio Astronomy and Ultraviolet Spectrometer instruments still return data, although the science teams are not supported. The only major instrument problems are the V1 PLS experiment, which no longer returns useful data, and the recent apparent loss of the V2 PWS wideband receiver. The V2 MAG experiment has had a continuing problem with noise generated by the spacecraft and other instruments making reliable analysis very difficult, but the increase in magnetic field strength at solar maximum has made that problem more tractable. Otherwise the instruments work well, and all have the sensitivity to continue observations in the environments expected beyond the TS and heliopause.

The sections which follow describe four broad science topics being addressed by the Voyager spacecraft. These topics are 1) the TS and possible precursors, 2) the environment beyond the TS in the heliosheath, 3) the interplanetary medium in the outer heliosphere, and 4) cosmic ray modulation. For each topic we give a description of the science, summarize recent results, and describe how Voyager data will be used in the future to advance our knowledge in these areas.

2. TERMINATION SHOCK

The TS is where the solar wind plasma makes its transition from super- to sub-magnetosonic flow. The solar wind plasma is compressed and heated and the magnetic field strength increases. Particles are energized at the shock. However, even basic parameters such as the shock strength and location are inferred only from modeling and simulation since estimates for

the LISM field strength vary from 0.05 to 0.5 nT. We expect to observe repeated crossings of the TS due to motions induced by a variable solar wind flow and magnetic field orientation. Multiple crossings should assist us in understanding the conditions governing the acceleration of energetic particles near the TS.

Models predict that the TS is a reverse, quasi-perpendicular ($Q_\perp$), collisionless shock at which the solar wind plasma is compressed and heated. Many studies have tried to predict the distance and character of the TS so that we could prepare for the encounters of V1 and V2 with the TS [*Stone*, 2001]. Theoretical models of the interaction between the heliosphere and the LISM have grown increasingly sophisticated [e.g., *Zank* (1999); *Fichtner* (2001); proceedings of The Outer Heliosphere: The Next Frontier, 2001]. These models incorporate complex and highly nonlinear phenomena, make quantitative, measurable predictions, and provide frameworks that enable one to visualize our heliosphere, and thereby gauge the present locations and future courses of the Voyagers on a global scale.

The TS probably accelerates the ACR component [*Pesses et al.*, 1981]. The acceleration process has been modeled using diffusive shock acceleration theory at a $Q_\perp$ shock. Recent studies at 1 AU [*Desai et al.*, 2003] shed new light on how $Q_\perp$ shocks accelerate particles from pre-energized seed populations, but much remains to be understood. Likewise, growing evidence suggests that shocks are not uniform, near-planar structures, but can possess significant curvature over short spatial scales [*Szabo et al.*, 2001]. Short-scale structure could lead to spatially-dependent particle injection and acceleration across the shock face in a manner that has yet to be fully appreciated. Simulations of perpendicular shocks show that they are unstable, with a cyclic overturning and reformation [*Quest*, 1985; 1986]. Indirect evidence for this process may exist in magnetic field observations of the Uranian shock [*Smith et al.*, 1989]. We do not know whether the TS is stable and, if not, how that would affect the injection of seed particles for acceleration [*Zank et al.*, 1996b].

As V1 enters the precursor region upstream (inside) of the TS and crosses the TS, quite possibly several times, we must be guided by past experience as well as by model predictions in properly assessing the implications of data from the various instruments. The Voyager spacecraft are tracked roughly 8-12 hours per day; thus, the probability of observing the shock itself at any particular crossing, including the first, is less than 50%. The Voyager spacecraft will probably not encounter the TS under quiet conditions. There are likely to be elevated populations of energetic ions and electrons from solar and interplanetary acceleration processes and significant variations in key solar wind plasma parameters due to large-scale disturbances (e.g., transient MIRs and global MIRs (GMIRs) and recurrent CMIRs). The time history of data from each Voyager records a single set of conditions in a complex and dynamic astrophysical plasma. Thus, we must be prepared for encounters with the TS and its upstream environs under conditions that modelers have neither considered nor could have anticipated. Accordingly, we must examine our data with open minds, lest our pre-conceived notions regarding a TS encounter conflict with, and unduly hamper, our discovering how such an encounter actually appears in the data.

2.1 Model predictions

Modelers generally study the TS assuming, for simplicity, ideal conditions (i.e., a quasi-stationary TS, relatively steady and uniform solar wind inflow, and low levels of non-thermal particles of solar and/or interplanetary origin). *Zank et al.* [1996a] compared model results for solar wind conditions at the TS with the *Mellott et al.* [1986] classification scheme for $Q_\perp$ shocks. They found that the effect of pickup ions was to increase the thermal pressure of the solar wind and decelerate the solar wind so that the predicted β (the ratio of thermal pressure to magnetic pressure) and magnetosonic Mach number M_F placed the TS into the turbulent, moderately supercritical (M_F>2-3) $Q_\perp$ shock regime. The strength of the shock is uncertain, with estimates ranging from 3-4 [*Linde et al.*, 1993] to as low as 1.9 for strongly pickup-ion and energetic-particle-modulated shocks [*Liewer et al.*, 1993; *Le Roux et al.*, 2000]. The energetic particles, including the ACRs created at the shock, can play a major role in weakening the shock [*Le Roux et al.*, 2000]; these upstream particles could also be observed as shock precursors at times of more radial magnetic field [*Liewer et al.*, 1995].

Le Roux et al. [2000] use a three-fluid model that self-consistently solves equations for 1) solar wind and low-energy pickup protons, 2) pickup protons accelerated by the multiply-reflected ion (MRI) process, and 3) protons accelerated to ACR energies by diffusive shock acceleration. They derive the differential proton intensity spectrum shown in Figure 2. Just beyond the shock the spectrum unfolds at lower energies, providing a clear signature of the shock crossing as shown by the top curve.

2.1.1 Plasma wave signatures

The Voyager plasma wave receivers should observe at least two signatures associated with the TS [*Kurth and Gurnett*, 1993]. Langmuir waves should be present

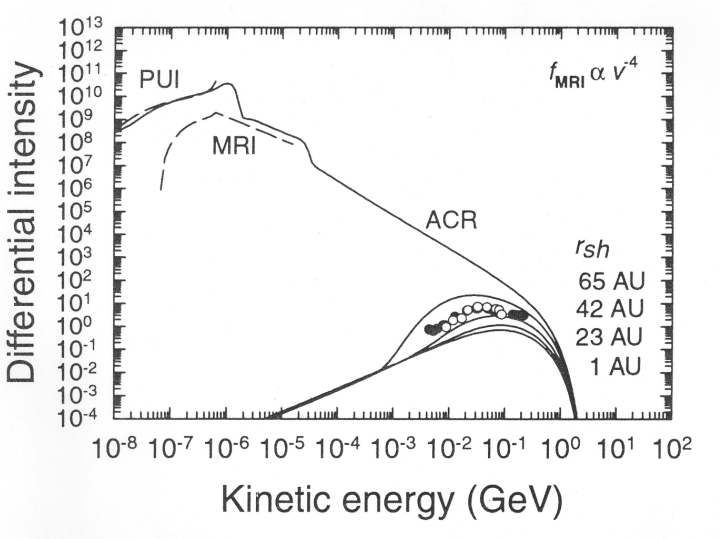

FIGURE 2. Differential intensities $m^{-2}s^{-1}sr^{-1}MeV^{-1}$ of protons predicted by the *le Roux et al.* [2000] model. The top solid curve (labeled r_{sh}) shows simulated unreflected pickup protons, MRI-accelerated pickup protons, and ACR protons immediately downstream of the TS at 86 AU. Lower solid curves show simulated ACR spectra at the indicated helioradii from 1 to 65 AU. Filled and open circles show measured ACR intensities at V1 (65 AU) and V2 (52 AU), respectively.

upstream of the TS. Depending on conditions in the vicinity of the shock, these waves could provide weeks of advanced warning of an impending shock crossing. *Macek et al.* [1993] extrapolated the Langmuir wave observations at the bow shocks of Earth and the outer planets to the TS and found field magnitudes of a few to a hundred $\mu V/m$, within the range detectable by Voyager. Langmuir waves associated with interplanetary shocks have been observed to distances of 65 AU; the waves at the TS should have much larger amplitudes.

Collisionless shocks are characterized by a relatively intense broadband burst of noise extending up to the electron plasma frequency. This noise provides one method of identifying the shock; the duration of the signature is related to the shock thickness and the relative speed of the spacecraft and the shock. Plasma wave turbulence at the bow shocks of Earth and the outer planets has been extrapolated to the TS by *Kurth and Gurnett* [1993]. If the TS had a strength similar to that of planetary bow shocks, plasma waves associated with the TS would have amplitudes in the range of 10^{-12} to 10^{-9} Vm^{-2} Hz, again detectable by the Voyager PWS receivers.

Another possible wave signature of the TS is weak narrowband radio emissions resulting from nonlinear interactions of the Langmuir waves generated in the foreshock region. These emissions have been detected at planetary bow shocks and at some interplanetary shocks. Given the lower intensities expected for Langmuir waves associated with the TS and the already low intensity of radio emissions associated with, for example, Earth's bow shock, radio waves from the TS will probably not be detectable with Voyager's relatively short antennas. Nevertheless, should such waves be observed, they would provide advanced warning of an impending shock crossing.

2.1.2 Magnetic field signatures

The MAG efforts to observe and identify the TS are focused on two endeavors: 1) Improved near-real-time diagnostics of possible shock crossings and 2) the first-ever measurements of the TS region. As discussed above, the TS is anticipated to be a $Q_\perp$ shock with a strength of ~2-3. The increase in the mean magnetic field intensity behind the shock will simplify the accurate measurement of the field. By analogy to interplanetary shocks and planetary bow shocks, we expect to observe a turbulent sheath region behind the TS. The levels of magnetic fluctuations in the sheath will be greatly enhanced over the upstream measurements. Near-real-time computations of the Pythagorean root-mean-square fluctuations level will provide a nearly error-free diagnostic of the TS crossing since these calculations are coordinate-system and zero-level independent and invariant. Thus the first penetrations of the heliosheath downstream of the TS should be readily identified even if the actual shock crossings occur during gaps in DSN tracking coverage.

2.1.3 Plasma and Particle Signatures.

The plasma bulk flow speed at the TS should decrease by a factor ~2-3, the density of the core proton distribution should increase by a comparable factor, and the proton and electron temperatures should increase. We expect to measure large variations about these nominal values in the turbulent heliosheath. For example, models predict large (factors of ~10 or more) density fluctuations as solar and interplanetary structures impinge on the TS [*Zank and Mueller*, 2003].

The LECP and CRS instruments on V1 and V2 should measure increased energetic ion and electron intensities as the spacecraft near the TS (see Figure 2). In particular, we expect the ACR energy spectra to fill in at increasingly lower energies, unrolling to power-law form. ACRs are believed to be accelerated at the TS [*Pesses et al.*, 1981]. Thus, upon crossing the TS or when magnetically connected to the TS, we should observe un-modulated ACR spectra. Also, based on our experience with transient and recurrent

shocks in the solar wind, we expect to measure angular distributions of energetic ions that display large, sporadic departures from isotropy. For example, at and near the TS, where particle drift acceleration occurs, we expect to observe unidirectional and bi-directional angular distributions due to ion and electron reflection from the TS and/or temporary trapping of such particles on IMF flux tubes that connect to the TS at multiple points, forming collapsing magnetic bottles.

2.2 New Upstream Phenomena at Voyager: Energetic Ion Intensities

Intense fluxes of energetic ions and electrons have recently been observed by the LECP and CRS instruments on V1. Figure 3 shows that from 2001 to 2002.5 the mean intensities of 2-3 MeV protons at V2 (~66 AU) are higher than those at the more distant V1 (~83 AU). The V2 observations are time-shifted to the location of V1 using the observed V2 solar wind speed. In mid-2002, the intensity of protons at V1 increased by a factor of ~100 with no corresponding increase at V2. These intensity increases are seen at energies from 40-4000 keV and have persisted for six months. A V1/V2 asymmetry this large over such a long time period is unprecedented in the Voyager observations.

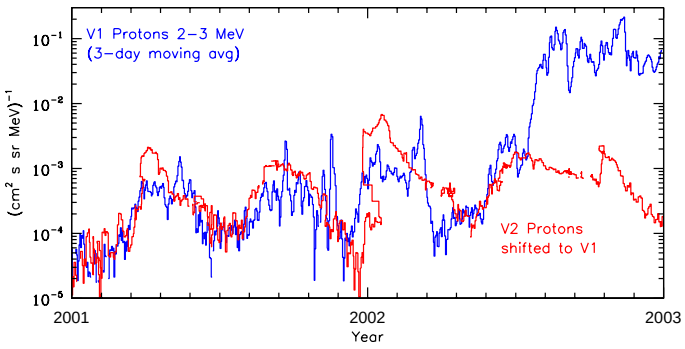

FIGURE 3. Intensity of 2-3 MeV protons during 2002 and 2003 at V1 and V2

Figure 4 shows energy spectra (open symbols) during four, seven-day time intervals which include the peak observed intensities. Spectra A-D are shifted to the right by logarithmic factors of 1-4, respectively. The solid circles show the average energy spectrum for the entire period 2002/210 to 2003/020. These spectra are remarkably flat and intense given the radial distances are $\geq$ 85 AU. Spectra for periods A, B, and C and for the event-average spectrum are well-fit by power laws, $j(E) \propto E^{-\gamma}$, with $\gamma = 1.46\pm0.05$, 1.36 ± 0.06, 1.34 ± 0.05, 1.46 ± 0.05, respectively. Spectrum D is not of power-law form, but has a slope of ~3/2 at low energy and steepens with increasing energy to a slope of ~2 at the highest energies (sample lines at the right of Figure 4 indicate four reference power-law slopes). Other ions, such as O, N, and Ne, also increased in intensity and developed a low-energy power-law component with spectral index near 1.5. For reference, if the power-law spectra were produced by shock acceleration, for $\gamma = 1.5$ DSA theory would imply a shock compression ratio $s = 2(\gamma+1)/(2\gamma-1) = 2.5$.

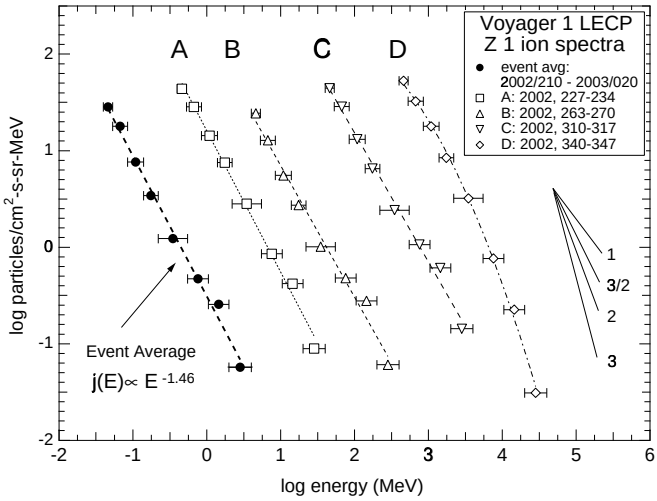

FIGURE 4. Energy spectra (open symbols) during four seven-day time intervals which include peak intensities. Spectra A-D are shifted rightward in energy by logarithmic factors 1-4, respectively, for clarity. The spectrum represented by solid circles is the event-average, covering the period 2002/210 - 2003/020. Horizontal bars on symbols indicate the channel energy-passband widths

These intense low-energy ions have very large flow anisotropies. Figure 5 shows 3-day averaged V1 LECP angular 0.57-1.78 MeV proton data for 2002. The orientation of the sectors is shown in the upper left. Intensities in each look direction are shown in color and the trace shows the total intensity. After the increase in intensity observed in mid-2002, the proton intensity peaks occurred predominantly in sectors 7 and occasionally 6. These results indicate that the energetic ions are headed outward from the sun along the nominal spiral IMF, which at these large distances is perpendicular to the radially outward plasma flow. The other energy and ion species channels on the LECP and CRS instruments also show intense flows away from the Sun with anisotropies as large as a factor of ten. Very large anisotropies are also observed during lower-intensity spikes observed prior to 2002.5 (for example, in the V1 spike at 2001.35 in Figure 3) and at V2. These strong anisotropies suggest that the spacecraft are not many mean free paths away from the acceleration site.

These data have led to conjecture that V1 entered the downstream region of a weak TS in mid-2002 and

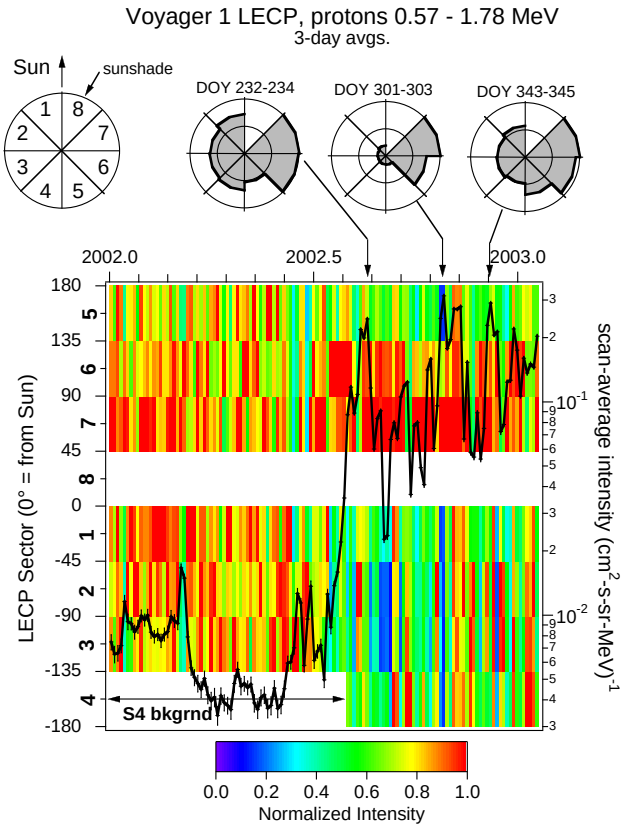

FIGURE 5. Angular data for 0.57-1.78 protons measured by V1 from 2002/001-2003/020. The color diagram shows 3-day averaged data, with time along the upper abscissa axis. The black trace shows the sector-averaged intensities. The pie charts at the top show the look directions and intensities at three locations.

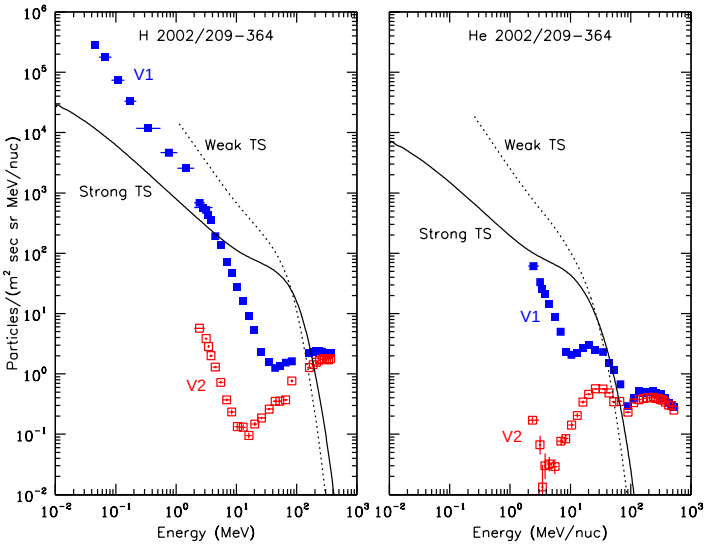

FIGURE 6. Energy spectra of H and He at V1 and V2 during 2002/209-364. Also shown are estimates of the energy spectra at the TS for two values of the shock strength.

that the outward flowing particles are those predicted to occur downstream of the TS. However, we do not agree with this scenario for several reasons. First, Figure 6 shows that the V1 ACR H and He spectra continue to show signs of modulation at energies ∼10-30 MeV/nuc. The figure shows the H and He spectra observed by V1 and V2 averaged over the latter part of 2002; the V1 intensity is 100 times that at V2. The GCR H and He have peak intensities at ∼200 MeV/nuc, while the ACR He that is accelerated at the TS has intensity peaks at ∼20 MeV/nuc. The lines show the predicted ACR intensities at the shock based on model fits to the ACR spectra observed during periods of minimum solar modulation [*Cummings et al.*, 2002a; b]. Predictions are shown for both a strong shock (solar wind speed drops by a factor of 4) and a weak shock (factor of 2.4 drop). The spectra have clearly not unrolled as would be expected at the TS crossing.

Second, ACE and Ulysses also observed hard energy spectra in the second half of 2002, with spectral indices essentially identical to those observed at Voyager. These observations suggest that the intensities at V1 may be composed, in part, of particles accelerated in the inner or middle heliosphere. Also, no magnetic field or plasma wave signatures of a TS crossing were observed. However, the origin of this new component is not understood.

2.3 Anomalous Cosmic Rays

The ACR ion species H, He, C, N, O, Ne, and Ar are interstellar neutrals that flow into the heliosphere, are ionized and become pickup ions [*Fisk et al.*, 1974], and then are accelerated by the TS. Taking into account the attenuation of the interstellar neutrals in the heliosheath, *Cummings et al.* [2002a; b] compared models of the neutral densities in the LISM [*Slavin and Frisch*, 2002] with the estimated fluxes of pickup ions at the TS. The model fluxes are in good agreement for H, He, N, O, and Ne. Comparison of the ACR relative abundances with these pickup ion fluxes indicates that the injection efficiency for diffusive shock acceleration increases with mass, reaching a plateau for masses of 14 to 20 amu. Using this injection efficiency for ACR Ar, the density of neutral Ar is estimated to be $(3.5 \pm 1.6) \times 10^{-7} cm^{-3}$ in the LISM, again agreeing well with *Slavin and Frisch* [2002].

Elements with low first ionization potentials, such as Na, Mg, Si, and S, are mainly ionized in the LISM and have significantly lower neutral interstellar densities. However, the ACRs of these species are much more abundant than predicted for such low LISM neutral densities, providing evidence for another source

of pickup ions in the outer heliosphere. Recently, *Schwadron et al.* [2003] proposed that the source of these minor species is small grains produced in collisions of Kuiper Belt Objects.

Using a drift model for acceleration and propagation of ACRs, *Cummings et al.*, [2002a; b] also estimated the source spectrum at the TS for each ACR species when the magnetic polarity A>0 (the field of the sun is outward in the northern hemisphere). Examples of the shock source spectra for H and He for a strong and a weak shock are shown in Figure 6. Models of shock drift acceleration predict that the intensity of the shock source at low latitudes will be higher during A<0 than for A>0 [*Jokipii*, 1986].

2.4 Cosmic Ray Electrons

In mid-2002, two of the V1 CRS cosmic ray telescopes observed a significant increase in the intensity of 2.5 - 70 MeV electrons that has persisted for 6 months. Prior to these observations, the telescope's response in the electron domain was dominated by the background produced by >1 GeV protons. The current intensity increases observed by V1 are statistically significant. The detailed pulse height data confirm that these particles are electrons. No electrons have yet been observed in the V2 data. The V1 electron intensity shows significant temporal variations that are correlated with changes in the flux of 2.5 MeV H and in the combined rate of 70-300 MeV H and >70 MeV/nuc He. By early 2003 the intensity had decreased but still remained above background levels.

The expected intensity of GCR 10 MeV electrons in the LISM is not well known. At 10 MeV, the predicted intensities from different models range over 2 orders of magnitude [*Strong et al.*, 2000]. *Langner et al.* [2001] prefer a value of 600 $m^{-2}s^{-1}sr^{-1}MeV^{-1}$; the peak value observed at V1 is 1 $m^{-2}s^{-1}sr^{-1}MeV^{-1}$. *Potgieter and Ferreira* [2002] modeled the transport of electrons within the heliosphere and found that the TS increases the intensity by a factor of about 2, that the contribution from Jovian electrons is negligible, and that significant electron modulation occurs in the heliosheath.

The V1 data are consistent with most of the modulation occurring in the heliosheath. No known interplanetary acceleration process could produce these electrons. Thus, the observations of 3-70 MeV electrons suggest that V1 is nearing the TS.

2.5 Future work

• Characterize the nature of the TS: determine the TS location, strength, and speed. Use this information to set limits on LISM parameters.
• Determine the abundances of all ACR species from H to Fe at the TS, look for new sources of ACR ions, and derive improved source abundances.
• Measure the unmodulated ACR spectrum and compare with acceleration models. Determine the shock strength $s = 2(\gamma+1)/(2\gamma-1)$, where the source spectrum is $dj/dE \propto E^{\gamma}$.
• Measure the GCR electron gradients across the TS.
• Characterize the plasma wave spectrum of the TS and compare it to that of interplanetary and planetary bow shocks.
• Monitor the intensity variations of low energy ions at V1 and V2 and correlate them with solar wind, magnetic field, and heliospheric current sheet data.
• Examine the connection between energetic particle intensities observed in the inner heliosphere and those observed in the distant heliosphere. Determine if the relatively small radial intensity gradient between the inner and outer heliosphere in late-2002 is indicative of ongoing acceleration processes (e.g., statistical acceleration) as ions are transported from the inner to outer heliosphere. Investigate these acceleration processes, try to understand how such hard energy spectra are maintained over such large spatial scales.
• Catalog the intense anisotropic energetic particle events and correlate the flow direction information with magnetic field data to try to determine the origin of these particles.
• Perform a Compton-Getting analysis on data from the V1/LECP lower-energy ion channels to estimate the solar wind flow speeds for the period starting in mid-2002.
• Compare GCR and ACR modulation for A<0 with A>0 observations. Look for evidence that the shock source intensity at low latitudes increases when A<0.

3. BEYOND THE TERMINATION SHOCK

For the past 25 years, the two Voyager spacecraft have traversed the supersonic solar wind with only momentary (albeit remarkable) passages through the outer planets' magnetospheres. Once Voyager crosses the TS and enters the inner heliosheath, however, a new phase of heliospheric exploration opens.

3.1 Heliosheath

The heliosheath is the region between the TS and the heliopause which contains shocked solar wind, perhaps analogous to the magnetosheaths of the planets. The plasma in the downstream region of the heliosheath is expected to be subsonic and its flow will

eventually turn from radial to tailward. The speed decreases at the shock from 300-700 km/s to 100-200 km/s and the magnetic field, density, and temperature increase. Thermal proton distributions in the magnetosheaths of all the outer planets except Uranus have two populations which are fairly well represented by Maxwellians, a thermal population with temperature of 100 eV which contains 50-70% of the proton density and a hot population with a temperature of 600-1000 eV comprising 30-50% of the proton density [*Richardson*, 2002]. Similar distributions could be present in the heliosheath, which would provide more clues as to their origin.

The heliosheath is unlikely to resemble the steady, rather pristine state suggested by steady-state models of the solar wind-LISM interaction. At least three effects are likely to be observed by Voyager:

1) The TS may be viewed as a "generator" of shocks and convected structures in the heliosheath. Detailed calculations and simulations show that any change in the momentum flux upstream of the TS will generate "N-shocks" propagating into the heliosheath, followed by convected tangential or contact discontinuities [*Zank and Mueller*, 2003]. Thus the heliosheath may well be even more dynamically active than the supersonic solar wind.

2) In and around the ecliptic region of the heliosheath, the azimuthal component of the interplanetary magnetic field (IMF), after being amplified by compression at the TS, will experience further amplification by the Axford-Cranfill effect. In addition, the field will be highly perpendicular. Since the field is convected slowly outwards through the heliosheath but is unable to cross the heliopause, the field will be compressed. Conditions at the heliopause could allow significant levels of reconnection; Voyager may therefore see reconnection-energized suprathermal particle populations.

3) Finally, it remains unclear what to expect of the heliospheric current sheet in the inner heliosheath. Simulations suggest that the current sheet may be highly unstable, leading to strong warping and movement away from the ecliptic [*Opher et al.*, 2002]. A narrow region of high speed flow could be associated with an unstable current sheet. The instability is analogous to a Kelvin-Helmholtz instability with wavelength scales of tens of AU. Thus the region near the current sheet may be unstable and dynamic. Given the modeled thickness of the heliosheath, Voyager will spend the better part of a solar cycle in transit, allowing for the study of the evolution of the heliosheath over a solar cycle.

Figure 7 shows the disruption of the heliosheath due to a GMIR propagating across the TS. The collision of the GMIR shock complex with the TS sets up a spatially enormous asymmetric ringing of the TS as it oscillates back and forth while gradually settling back into its original location. The forward shock propagates at an approximately constant speed upstream of the TS and the weaker reverse shock trails. The forward shock transmitted through the TS slows dramatically and the TS is driven outward by a maximum of 3 AU at the nose. The TS then recovers and moves inward, and shortly thereafter encounters the reduced ram pressure of the reverse shock. This causes the TS to accelerate inward, moving as far as 5 AU inside its original position, and heat the solar wind even more. As a result, a region of heated subsonic solar wind is produced and convects slowly away from the TS. Finally, the GMIR propagates very slowly into the shocked LISM. A reverse shock follows the leading forward shock into the LISM, and in principle, both could be responsible for the radio emission observed by the Voyager spacecraft. The TS relaxes to equilibrium in about 670 days. This scenario is repeated to a greater or lesser extent for every solar wind structure colliding with the shock. Since the recovery time from the GMIR collision, ~670 days, is much longer than the observed time between MIRs at 70 AU (about 90 days), the heliosheath should be in a continuously disturbed state.

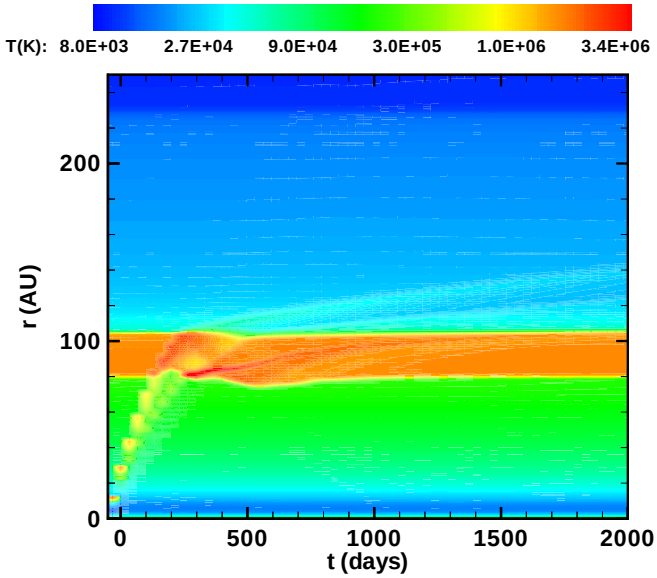

FIGURE 7. Space-timeplot of the plasma temperature along the stagnation axis illustrating the response of the TS (80 AU) and heliopause (103 AU) to a shock of global extent.

If the V1 PLS cannot measure plasmas in the heliosheath, we can estimate the flow speed V1 before, during, and after the TS encounter by analyzing the angular distributions of low-energy, 40 to 4000 keV, ions with charge states Z>1 and of 0.6-1.8 MeV protons measured by the LECP instrument. We will use

the Compton-Getting anisotropy to extract the speed from the arrival directions of low-energy ions. This method has provided accurate speed estimates in planetary magnetospheres and in the solar wind [*Kane et al.*, 1998].

In the heliosheath the spacecraft will encounter enhanced and highly variable intensities of energetic charged particles. The particle distributions will be admixtures of: (1) solar wind plasma heated by the TS and the solar wind superthermal tail accelerated by the TS; (2) energetic particles incident on, accelerated at, and convected downstream of the TS; (3) particles accelerated by heliosheath shocks, resulting from solar wind structures impacting the TS, and by statistical processes mediated by enhanced heliosheath plasma turbulence; and (4) other new sources.

Component (2) will include pickup ions, remnant solar energetic particles from transient events (flares, CMEs), particles accelerated between the sun and the TS by transient, MIR- and GMIR-driven shocks, by quasi-recurrent (~26-day) CIR- and CMIR-driven shocks, and by statistical processes, such as transit-time damping and Fermi-II, in the turbulent, supersonic solar wind plasma [e.g., *Zank*, 1999; *Fichtner*, 2001]. Component (3), which one expects to be highly dynamic, is of particular interest since it is the product of acceleration processes operative in a stellar plasma sheath in an extreme state of agitation, a condition that astrophysical data would indicate is not unusual. Ion and electron spectral and angular data and ion compositional data will provide insight into the spatial and temporal variations of injection and acceleration processes at the TS, and should also reveal how transport processes through the heliosheath modify the particle distributions.

Turning to the highest energy particles, the GCRs, V1 will encounter a completely different and as yet unexplored modulation regime in the heliosheath; a region where adiabatic deceleration and drift effects should not be important, and diffusion-convection processes in a highly turbulent medium should dominate. As described in Section 5, over 85% of the GCR modulation occurs outside the TS, most likely in the heliosheath. If the modulation occurs in the heliosheath, the heliosheath must have large radial GCR intensity gradients (>3%/AU for 265 MeV/nuc GCR He). Voyager will be able to measure these gradients and the environment which produces them.

Given the expected dynamic nature of the heliosheath and the numerous sources of energetic particles, plasma waves should play a role in mediating the flow of energy between the various particle populations. In particular the PWS should observe Langmuir waves generated upstream of shocks propagating through the subsonic solar wind and broadband electrostatic waves at the shocks. These waves, although weak, are still occasionally observed in the supersonic solar wind at strong interplanetary shocks.

Numerous theoretical factors suggest that the inner heliosheath should be a highly dynamic region on almost all possible scales. Voyager will provide considerable insight into this wholly mysterious region, revealing for the first time some hint of the very complicated physical processes that govern the interaction of the solar wind and the LISM. These data will in turn provide us with our first insights into the coupling of stellar winds with the interstellar medium.

3.2 Heliopause and Interstellar Medium

As the Voyagers begin their trek through the uncharted heliosheath, the next mile post in their voyage will be the heliopause. One possible heliopause signature is the low-frequency (1.8-3.6 kHz) radio emissions detected by the Voyager PWS instruments and shown in Figure 8. These emissions are generated at or beyond the heliopause, possibly by transient solar wind shocks associated with GMIRs interacting with the LISM.

A recent compilation of information on the location of the source of these radio emissions [*Kurth and Gurnett*, 2003] shows that they lie in the general direction of the heliospheric nose along a line roughly parallel to the galactic plane (Figure 9). A possible explanation for this linear formation of source regions is that the orientation of the interstellar magnetic field may control the emission of the radio waves, although the details of how this works are not understood. Inferences of the galactic magnetic field via the polarization of starlight and rotation measures of pulsars indicate the ordered galactic field is parallel to the galactic plane, hence, the radio source regions may reflect this field orientation in the LISM.

Two major radio emissions events have been observed to date, with onsets in 1983 and 1992 during the declining phases of the last two solar cycles. Late in 2002 a new radio emission event was observed, the first radio activity since mid-1996. This emission, the transient event in late 2002 shown in Figure 8, is similar to the weak transient events which heralded the major radio events of 1983 and 1992. Recent attempts to predict the onset of radio emissions [*Wang et al.*, 2001b; *Zank et al.*, 2001] based on shock arrival times at the heliopause [*McNutt*, 1988] have failed; hence, many questions remain about how the radio emissions are triggered and their generation mechanism. Observations of solar wind structures evolving through the heliosheath may shed light on which structures trigger the heliospheric radio emissions.

While it is by no means assured the Voyagers will survive to the heliopause, we must look forward to this

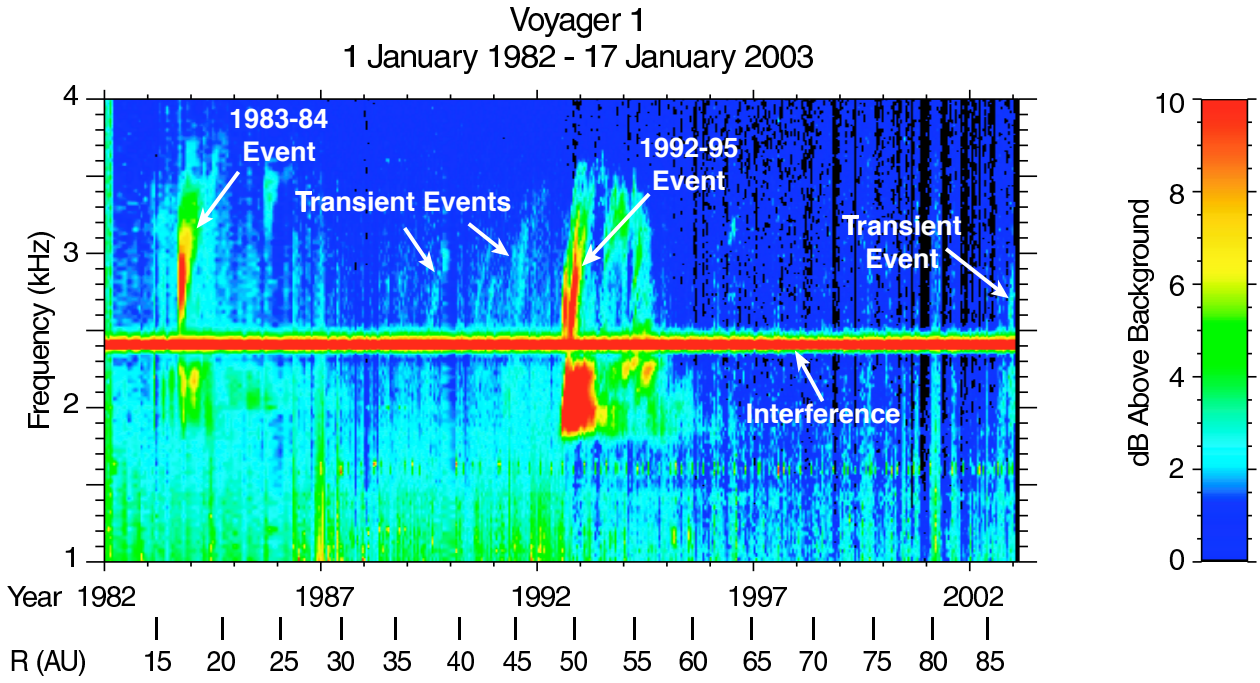

FIGURE 8. PWS spectra showing heliospheric radio emissions.

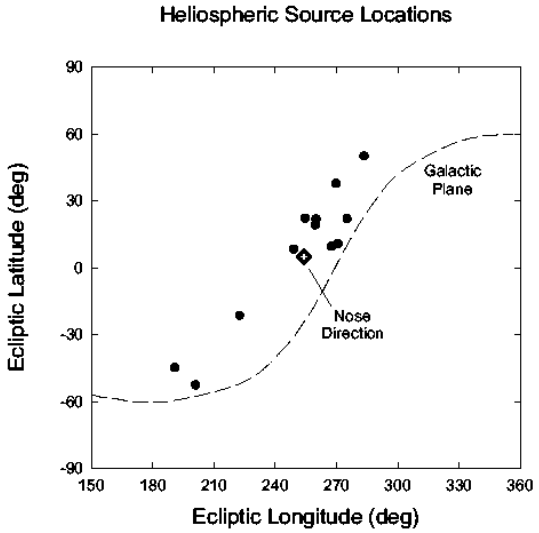

FIGURE 9. Locations of the source of the heliospheric radio emissions.

possibility. This passage will be humankind's first step beyond the heliosphere into interstellar space and the Voyagers will truly become interstellar probes. They will either measure the direction and magnitude of the interstellar magnetic field or set an upper limit of roughly a half of a microgauss to the field. We will be able to assess the extent to which the outer heliosheath modulates GCRs. We will make the first measurements which expose the extent to which the heliosphere influences the LISM, whether or not turbulence is present in the immediate upstream LISM, and the flux of ACR's leaving the heliosphere. We will measure the low-energy part of the galactic ray spectrum for the first time. We will, perhaps, observe the source of low-frequency heliospheric radio emissions directly. The measurement of the magnetic field will give us the Alfven speed, so we will determine whether a bow shock precedes the heliosphere. We may find whether structures propagate through in the LISM and, if so, their nature, where they come from, and what they tell us about the evolution of the interstellar medium and its interaction with astrospheres of stars.

3.3 Future work

- Characterize the heliosheath environment.
- Observe the next episode of the heliospheric radio emissions and try to correlate structure in the emissions with solar wind conditions.
- Continue modeling efforts to understand the dynamics of the heliosheath.
- Observe the properties of cosmic ray modulation in the heliosheath.
- Characterize the heliopause and LISM and how they are affected by the heliosphere.

4. MATTER AND MAGNETIC FIELDS IN THE DISTANT HELIOSPHERE

The Voyager spacecraft are advancing through an unexplored region of the heliosphere. The medium through which they move contains plasma that originates in the Sun, neutral particles that originate in the LISM, magnetic fields, low-energy charged particles, and dust particles. The Sun and the interstellar medium are competing for dominance of the medium. Interstellar neutral particles penetrate deeply into the heliosphere, but the Sun and solar wind ionize them, turning them into hot pickup ions which are carried back into the LISM by the heliospheric magnetic field. In the distant heliosphere, where the Voyager spacecraft are now, the solar material dominates the momentum of the medium, but the interstellar pickup protons dominate its internal pressure. This medium is a unique state of matter that has not been produced on Earth, but which does exist in many places in the universe. The distant heliospheric medium has a rich structure that is produced both by the nature of the emissions of material and magnetic fields from the Sun and by dynamical interactions. During the last few years, the structure of the medium through which the Voyagers passed was related to the complicated solar conditions associated with the maximum phase of the solar cycle. During the next few years the structure of the medium explored by the Voyagers will be related to relatively simple conditions associated with the declining phase of the solar cycle. The next solar minimum is expected to occur in 2006 or 2007.

4.1 Solar Wind Slowdown

The solar wind slows down as it moves from the Sun to the distant heliosphere. The solar wind plasma ionizes the interstellar neutrals, which then are accelerated to the solar wind speed and heated to a thermal energy equal to the solar wind energy, about 1 keV. The energy for this acceleration and heating comes from the bulk motion of the solar wind; thus the solar wind should slow down if sufficient pickup ions are entrained in the flow. Knowledge of the speed decrease provides an estimate of the number of picked-up interstellar neutrals, and thus of the interstellar neutral density. Determination of the solar wind deceleration requires a difference measurement between the solar wind speed in the inner heliosphere (at Ulysses or a spacecraft near Earth) and at the distance of V2. Magnetohydrodynamic (MHD) modeling is used to predict the speed expected at V2 based on solar wind parameters in the inner heliosphere, then the density of the interstellar H is adjusted so that the model results match the observations. These calculations can be performed only when two spacecraft are at the same heliolatitude or near solar maximum, when heliolatitudinal speed gradients are small.

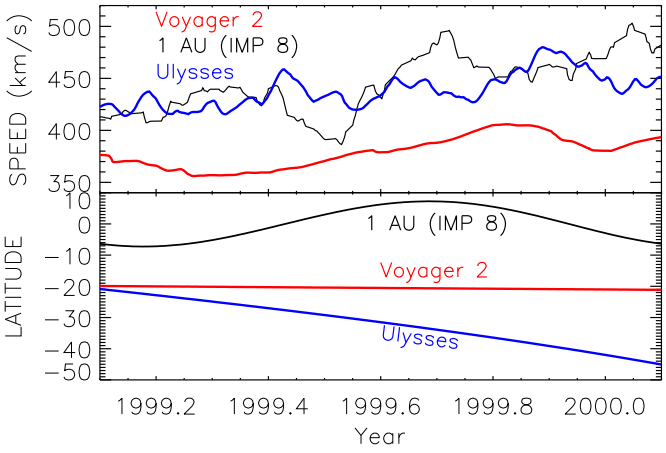

FIGURE 10. The top panel shows solar wind speeds observed at 1 AU, Ulysses, and V2 in 1999-2000 time-shifted to 1 AU using the observed speed at each spacecraft. The bottom panel shows the heliolatitudes of each spacecraft. V2 sees speeds which are lower by about 50 km/s.

Figure 10 shows a plot of speeds observed by Wind, Ulysses, and V2 (time-shifted to 1 AU to facilitate comparison) and the latitude of these spacecraft. At solar maximum, latitudinal gradients of the solar wind parameters were small [*McComas et al.*, 2000]. Wind and Ulysses, at low and high heliolatitudes, respectively, see very similar solar wind speeds. V2, at an intermediate latitude, observed much lower speeds. Using a 1-D MHD model, *Wang and Richardson* [2003] showed that the speed at V2 was 12-14% below that expected in the absence of pickup ions and that this slowdown implied an interstellar H density of 0.09 cm^{-3} at the TS. As the solar wind moves farther out the deceleration should increase: the next opportunity to estimate the speed decrease will be in 2006, near solar minimum, when both Ulysses and V2 will be at 26° S heliolatitude.

4.2 Temperature Increase

The pickup ions are hot compared to the solar wind protons, and some of that energy can be transferred to the thermal protons. Figure 11 shows 50-day running averages of the temperature of the solar wind plasma (black line). The plasma temperature decreases from 1 to about 30 AU, then increases. The adiabatic temperature profile is shown by the green line; the observed temperatures are well above this line, so significant heating of the solar wind occurs. *Smith et al.* [2001a] modeled the solar wind temperature profile; roughly 5% of the energy available from the relaxation

of pickup ions from a pickup (cylindrical) distribution to a shell distribution cascades to the thermal protons. Their model gives the blue curve in the figure, which reproduces the general shape of the data but not the detailed structure. *Richardson and Smith* [2003] added a linear speed-temperature dependence to the Smith et al. model, and obtained the red curve, which reproduces the observations well. They show that the same speed-temperature relation fits the data from IMP 8 at 1 AU.

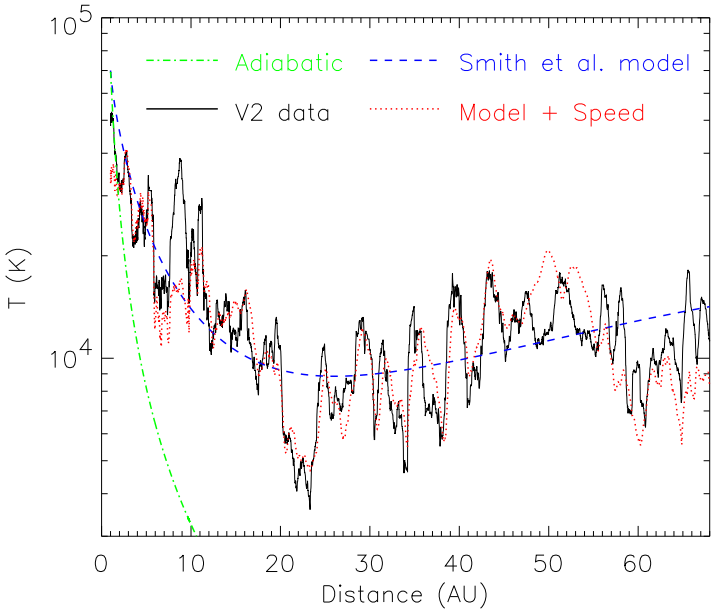

FIGURE 11. 101-day running boxcar averages of the V2 temperature (black line) versus radial distance, the adiabatic profile (green line), the *Smith et al.* [2001] model result (blue line), and a superposition of the *Smith et al.* [2001] model and a speed-temperature relation (red line).

This result is curious since the relationship in the outer heliosphere cannot be a relic from the inner heliosphere, because almost all the energy of solar wind protons results from heating processes. Thus this result implies that the heating rate is a linear function of temperature. We will work to understand this heating relation. A first step will be to run the Smith et al. model with varying input speeds to see if that can reproduce the detailed observed structure; if not, we will investigate other possible heating mechanisms.

4.3 Radial Variations of the Magnetic Field

Parker [1958] predicted that the IMF would have a spiral structure, and he predicted how the intensity of the IMF would vary with increasing distance from the Sun. His equations show that the IMF field strength (B) depends parametrically on the solar wind speed and on the strength of the magnetic field near the Sun, both of which vary with the solar cycle. The Voyager observations of B made over the past 25 years from 1 to 81 AU are in agreement with Parker's prediction [*Burlaga and Ness*, 1993; *Burlaga et al.*, 2002a]. We propose to continue to observe the radial variation of B and compare it to the predictions of Parker.

Sectors, alternating regions of sunward and antisunward magnetic field, are observed at 1 AU throughout the solar cycle [*Ness and Burlaga*, 2001]. At 1 AU, two (or four) sectors per solar rotation recur from one rotation into the next. Between 1999 and 2002, V1 and V2 observed sectors, but saw no regular sector pattern [*Burlaga et al.*, 2003a]. The heliospheric current sheet was evidently severely distorted by transient ejecta and the interactions among flows as they moved through the heliosphere. During the declining phase of the solar cycle, a sector pattern is generally clear at 1 AU and extends to relatively high latitudes. We propose to search for sectors and a sector pattern in the V1 and V2 data during the next few years of declining solar activity. We will model the evolution of sectors and the sector pattern from 1 AU to the positions of V1 and V2.

4.4 Recent Plasma Observations

Hourly averages of the solar wind speed, density, and temperature observed by V2 in 2001 and 2002 are shown in Figure 12. The speeds range from 320 to 470 km/s, the densities from 2×10^{-4} to 6×10^{-3} cm^{-3}, and the temperatures from 2,000-60,000 K.

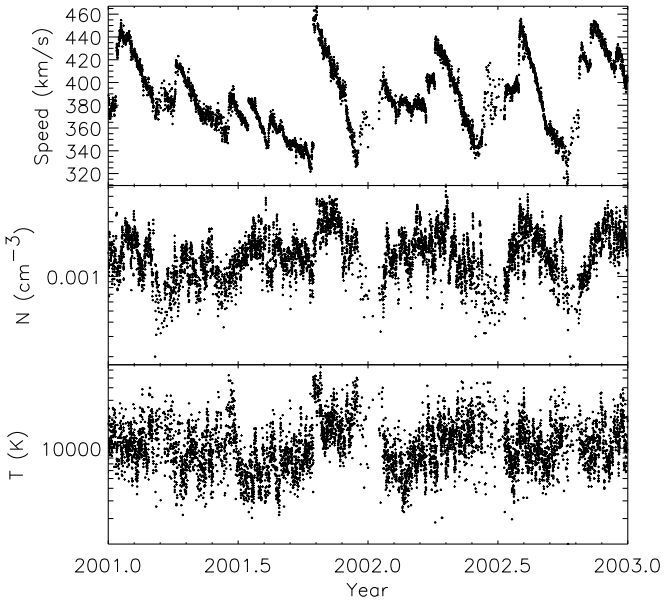

FIGURE 12. Recent solar wind plasma hourly-average speeds and densities.

The solar wind has recently been characterized by simultaneous increases in speed and density occurring every four months, followed by more gradual decreases in these quantities. The correlated change in density and speed over scales of months is a solar wind feature not observed previously; if one plots yearly correlations of daily averages of speed and density, one finds a strong negative correlation near 1 AU, almost no correlation from 5 - 65 AU, and a positive correlation during the most recent two years. The positive correlation of speed and density results in large pressure pulses, which should affect the TS motion. We will determine whether this positive correlation extends throughout the declining phase of the solar cycle, and we will model the correlation as a function of distance from the Sun.

4.5 Multi-scale Statistical Structure of the Large-Scale Magnetic Field and Plasma Fluctuations

On scales of the order of several solar rotations, streams, MIRs, GMIRs, and other similar structures have the nature of large-scale fluctuations. *Burlaga et al.* [2002c, 2003b] introduced a multi-scale statistical approach to describe and model the radial evolution of these fluctuations at various epochs of the solar cycle. The fluctuations of the interplanetary magnetic field strength (B) and the solar wind speed (V) are described by multi-scale statistical functions derived from measurements made by a spacecraft over the course of a year. The functions include: the multi-scale probability distribution functions, structure functions, the multi-fractal spectrum, the power spectral density spectrum, and multi-scale measurements of the standard deviation, skewness, and kurtosis. The properties of V and B near solar maximum and during the declining phase of the solar cycle were described by *Burlaga et al.* [2002c, 2003b; c; d]. These authors found good agreement between the measured multi-scale functions and those predicted by a multi-fluid MHD model [*Wang and Richardson*, 2002, 2003; *Wang et al.*, 2000] using the ACE observations at 1 AU as input.

Burlaga et al. [2003c, d] predicted the multi-scale structure of B and V that will be observed by V2 during the next few years. We propose to compare these predictions with the observations and extend the use of multi-scale statistical methods to describe the state of the solar wind and its evolution from 1 AU to the very distant heliosphere. We will extend the multi-scale statistical approach to describe the density and temperature structure and to study the correlations among the large-scale fluctuations in B, V, N, and T.

4.6 Coronal Hole Flows in the Distant Heliosphere

The next few years will mark the transition from solar maximum to solar minimum. The previous declining phase was marked by corotating structure; shocks were observed roughly once/solar rotation although the energetic particle intensity increases were usually a few days behind the shocks [*Lazarus et al.*, 1999]. In the current data, about 30 AU further out, very few structures repeat on solar rotation time scales; instead, the structure size is roughly 90 days. We will model the evolution of the solar wind using a MHD model with pickup ions to try to understand the merging process that creates this structure.

Previous studies have shown that during the declining phase of the solar cycle, the solar wind at 1 AU is dominated by corotating streams, which give way to interaction regions that merge and dominate the region between several AU and 30 AU. V2 data show that during 1994 and 1995 the transition of the solar wind from order to chaos occurred near 30 AU. The relatively simple corotating merged interactions near 10 AU were not observed at 75 AU. At the larger distances, V2 observed jump-ramp speed structures and relatively small fluctuations in the magnetic fields. We shall determine how these speed and magnetic field structures evolve beyond 55 AU. We shall test the prediction that the distribution of the strongest magnetic fields is approximately exponential.

4.7 Radial Evolution of Shocks and Transient Ejecta

We have had excellent success in understanding the evolution of shocks and CMEs from the inner to outer heliosphere near solar maximum. The Bastille Day shock occurred when Earth and V2 were at nearly identical heliolongitudes. Using observations at 1 AU as input, an MHD model that included pickup ions was able to predict the shock arrival time at V2 to within a few days and predict the speed jump almost exactly [*Wang et al.*, 2001b]. The observed enhancement of the magnetic field strength at V2 [*Burlaga et al.*, 2001] was also predicted by *Wang et al.* [2001a]. The structure observed at V2 resulted from the interaction and merging of several events observed at 1 AU [*Whang et al.*, 2001; *Zank et al.*, 2001].

The October 2002 shock observed at V2 was also reproduced very accurately starting with 1 AU data. In this case, the shock resulted from the merging of multiple solar events which spanned nearly a solar rotation [*Wang and Richardson*, 2002].

CME ejecta were traced from Ulysses to V2 using the enhanced alpha particle fraction, a characteristic

of some CMEs, as a marker [*Paularena et al.*, 2001]. Alpha particle enhancements were also used to trace the development of a MIR from a CME on the Sun to an enhanced magnetic field and density region at V2 at 58 AU [*Richardson et al.*, 2002]. The solar maximum regime is, however, a fairly benign one for tracking events outward, dominated by large CMEs and with little latitudinal structure. We will continue modeling solar wind evolution using MHD models to see if they can reproduce the observations in a solar wind dominated by interacting streams in the declining phase and by bipolar flows near solar minimum. Success or failure of the modeling will tell us if the relevant physics is included in the models.

4.8 Solar Minimum and Shear Flows

At the last solar minimum, V2 was at 16 ° S heliolatitude and saw a peak speed of only 570 km/s, indicating that V2 did not enter the fast coronal hole flow but remained in the transition region between slow and fast solar wind. This result was consistent with the estimate that the half-width of the slow wind region was about 15° in 1996 [*Paularena and Richardson*, 1997]. At the next solar minimum, V2 will be at 26° S heliolatitude and should enter the high-speed solar flow. This event will provide a unique opportunity to investigate the evolution of the fast solar wind. Of particular interest will be the temperature. Since the fast solar wind speed is nearly constant, much less stream interaction/shock heating should occur and most of the proton energy we observe should be from the interaction with pickup ions. V2 should also spend an extensive period within the velocity shear zone, the transition between the fast and slow solar wind regimes. The velocity shear, together with compressive effects, may produce a heliospheric vortex street [*Burlaga*, 1990; *Goldstein et al.*, 2002]. The vortex street would produce oscillating North-South flows with a period of about 26 days such as those observed in the Voyager data during the past two solar minima [*Lazarus et al.*, 1988; *Burlaga and Richardson*, 2000]. The velocity shear may operate to mix the fluids, particularly since the stabilizing influence of the field is reduced when the magnetic field is perpendicular to the velocity. In that case, we would expect a turbulent region, with perhaps substantial heating of the plasma and energetic particles. Since Ulysses will be at the same southern latitude as Voyager at this time, we will have an opportunity to see how the shear regions evolve from 4 to 75 AU.

4.9 Low Energy Particle Transport and Acceleration

V1 and V2 continue to observe increases of energetic ion and electron intensities in association with shocks. The remarkable activity at V1 beginning in mid-2002 is discussed in Section 2. Here we focus on recent data from V2, on which the PLS instrument is operating normally and provides crucial data on plasma variations. Figure 13 shows plasma and energetic ion variations at V2 during 2000.8 - 2003.1 (62.2-69.4 AU, 22°-24°S heliolatitude). Dashed vertical lines indicate three shocks that had marked effects on low-energy ion populations. Panel (a) contains hourly-averaged solar wind speeds from the PLS instrument. Panels (b) and (c) contain LECP proton data in three differential channels spanning 0.5-30 MeV and in one integral channel, >70 MeV.

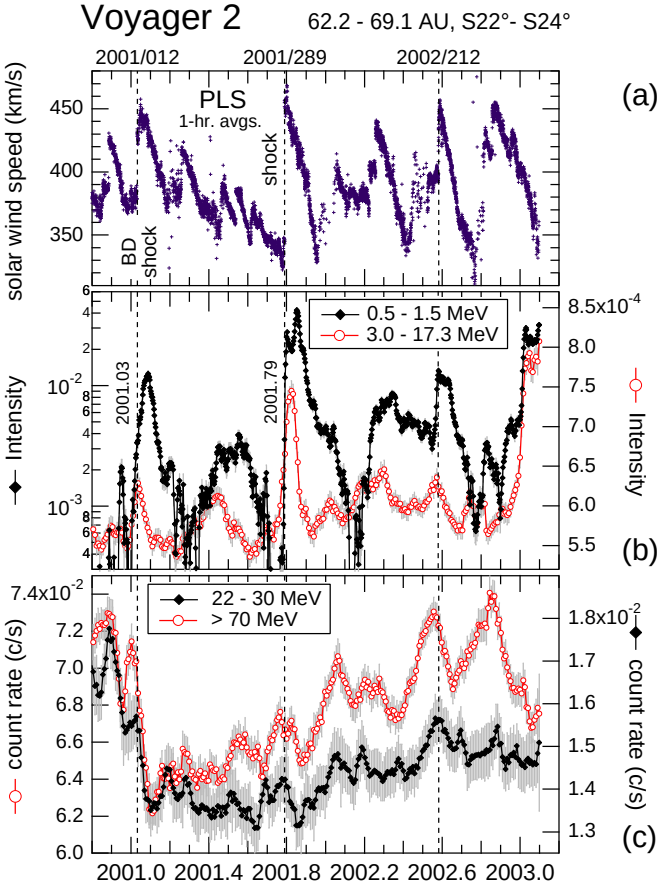

FIGURE 13. Shock-associated variations in solar wind speed and energetic proton intensities at V2 during 2001-2003

The shock at 2001.03 is driven by the MIR associated with the Bastille Day (BD) 2000 geomagnetic storm and other ejecta from intense solar activity in mid-July 2000. Intensities of both the 0.5-1.5 and 3-17.3 MeV protons began rising 10 days prior to pas-

sage of the BD shock. The peak intensity of 3-17.3 MeV protons coincided with the shock arrival, but the 0.5-1.5 MeV proton peak occurred 20 days later. The 22-30 MeV and >70 MeV proton intensities were depressed by the passage of the increased magnetic field in the MIR.

The shock at 2001.79 was stronger than the BD shock and the shock passage was detected by the PWS instrument as a broadband noise burst. Ion intensity increases associated with the passage of this shock extended from 28 keV to 10 MeV, were factors of 5-10 larger than for the BD shock, and displayed significant energy-dependent spatial structure [*Decker and Krimigis*, 2003]. The pre-shock intensity increase of 0.5-1.5 MeV protons was only two days wide, while that of the 3-17.3 MeV protons was about 12 days wide. The 0.5-1.5 MeV protons have large intensity peaks 5 and 25 days after the shock passage, while the 3-17.3 MeV proton intensity peaked 15 days after the shock and then dropped rapidly.

We examined the Z>1 ion energy spectra in eight energy channels from 28-3500 keV during the 5-day period from 2001.800-2001.814 behind the 2001.79 shock (this period includes the first post-shock peak of 0.5-1.5 MeV protons in Figure 13(b)). The energy spectrum is well fit by a power-law in energy with spectral index $\gamma = 2.1$. The spectral exponent predicted by DSA theory is $b = (s+2)/2(s-1)$, where s is the plasma compression ratio across the shock. This prediction is applicable for steady-state acceleration at a planar shock. The plasma density increased across the shock by a factor of about two, so b~2 and the observed power-law spectral exponent is consistent with that predicted by DSA theory.

The shock on 2002.58 produces pre-shock proton intensity rises that increase in duration with energy. These particles may consist of an ambient proton population that has been magnetically reflected by and swept ahead of an outwardly propagating, large-scale disturbance bearing an enhanced magnetic field, such as an MIR. Note that such structure is not always observed ahead of MIRs (e.g., the 2001.79 MIR). Only the 0.5-1.5 MeV protons maintain a post-shock intensity elevation, which persists for about 20 days.

4.10 Proton Anisotropies

Low-energy proton intensities in Figure 13(b) are enhanced from late 2002 through 2003.1. These elevated intensities are not shock-related, but occur during a period of largely unstructured, monotonically decreasing solar wind speed and exhibit large, non-convective, anisotropies. Figure 14 shows 5-day averages the 0.5-1.5 MeV proton channel data from 2002.95-2003.1. The orientation of the sectors (described in Section 2) is indicated by the inset in the upper left.

The main panel in Figure 14 shows the time evolution of count rates in sectors 3, 7, and the average over all seven active sectors. The two pie plots at the top show the relative count rate in the seven active sectors for two 5-day periods. During the (still evolving) period of elevated intensity in Figure 14, more protons were arriving in sectors 6 and 7 than in sectors 2 and 3. In other words, protons were moving preferentially away from the sun along the azimuthally directed heliospheric magnetic field. Such anisotropies are unusual. The absence of a local disturbance in the PLS data plus the arrival direction of the protons suggest that the protons originated from a non-local source lying sunward of the spacecraft. In addition, conditions in the solar wind plasma between the source and the spacecraft must have been such that field-aligned anisotropies could be maintained, i.e., the transport involved weak scattering.

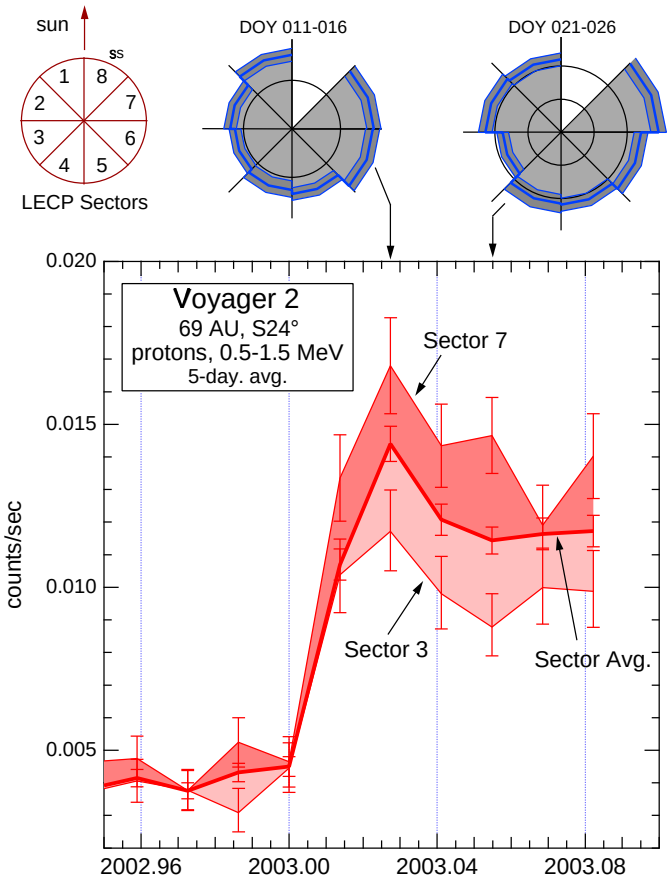

FIGURE 14. Anisotropic angular distributions of 0.5-1.5 Mev protons observed at V2 during early 2003.

4.11 Dust

A nearly steady rate of about 5 dust impacts per hour (normalizing for the small duty cycle of the waveform measurements) has been detected by the PWS instruments in the outer heliosphere [*Gurnett et al.*, 1997]. The electric field waveforms of these dust impacts are very similar to the waveforms detected from dust impacts near the ring plane crossings at the outer planets [*Gurnett et al.*, 1983; 1987; 1991]. The impulsive dust impact waveforms are produced by an impact ionization effect when a high velocity particle strikes the spacecraft body. At the very high velocities involved, greater than 20 km/s, the particle is instantly vaporized and heated to a very high temperature, about 10^5K, thereby producing a small, rapidly expanding cloud of gas. As the plasma cloud sweeps over the PWS electric antenna, it produces a voltage pulse. The size of the impacting particles is thought to be on the order of 1 micron since the waveforms are similar to those produced by impacts near Saturn's G ring, which is composed of micron size particles. The impact rate has been nearly constant from well inside the orbit of Saturn, where the particles were first identified, to 86 AU and is essentially the same at both V1 and V2. Since the impact rate shows no tendency to decrease with increasing radial distance from the Sun, the particles are probably not of planetary origin. The leading possibilities are that they originate from interstellar space or from distant solar objects, such as those in the Kuiper belt. Since the Kuiper belt objects are relatively close to the ecliptic plane, continued observations as the spacecraft move farther from the ecliptic plane should eventually allow us to determine if they originate from the Kuiper belt.

4.13 Future Work

• Determine the speed decrease observed at V2 when Ulysses and V2 are at the same latitude in 2006. Compare with models to see if the slowdown results from energetic particle interactions in addition to pickup ions.
• Try to model the heating mechanism which produces the observed speed-temperature correlation.
• Observe how the sector structure of the magnetic field evolves at intermediate latitudes at large distances. Compare observations of the magnetic field with Parker's predictions.
• Expand the use of statistical descriptions of the solar wind; compare the predictions of these descriptions with observations.
• Characterize coronal hole solar wind at large distances: determine cooling rate and pickup ion energy input by comparing with Ulysses data.
• Observe the latitudinal region where fast and slow wind mix; look for evidence of particle acceleration in these turbulent regions.
• Determine if vortex streets can be observed at solar minimum at 70 AU.
• Use models to track events from the inner heliosphere to Voyager under the more challenging conditions nearer to solar minimum. Observe how CIRs and CMIRs evolve at large distances.
• Compare plasma and low-energy ion intensity data from V2 to characterize shock acceleration processes in the distant heliosphere.
• Use observations of quasi-recurrent (i.e., CMIR-associated) ion events at V2 during the next solar minimum to study pickup-proton mediated weakening of recurrent shocks [*Decker et al.*, 2001].
• Characterize and try to understand the outward flowing particle fluxes observed on both V1 and V2. Use these data to learn about transport processes (e.g., weak pitch-angle scattering) in the outer heliosphere [*Decker et al.*, 2000].
• Monitor how the rate of dust impacts changes with heliolatitude.

5. COSMIC RAY MODULATION

The termination shock is the gateway to understanding GCR modulation. The Voyager cosmic ray observations, which span more than a complete heliomagnetic cycle and extend beyond 87 AU, have radically changed our concepts of cosmic ray modulation in the heliosphere. The analysis of those data combined with those from 1 AU and from Pioneer 10 shows that:

1) At solar minimum during A>0 epochs, most of the GCR modulation occurs at or beyond the TS. To a lesser extent, this statement is also true during A<0 solar minima.

2) The reduction in cosmic ray intensity from solar minimum to solar maximum occurs mainly beyond 15 AU.

3) Inside 15 AU, the longterm changes in the transport parameters over a heliomagnetic cycle are much smaller than in the outer heliosphere.

4) Galactic cosmic rays appear to be reaccelerated at the TS.

These observations do not require changes in the Parker transport equation. The basic physical processes involved in cosmic ray modulation, diffusion, convection, adiabatic energy losses and gradient and curvature drifts in the large-scale structure of the interplanetary magnetic field, are still valid. What is missing is our knowledge of the temporal and spatial

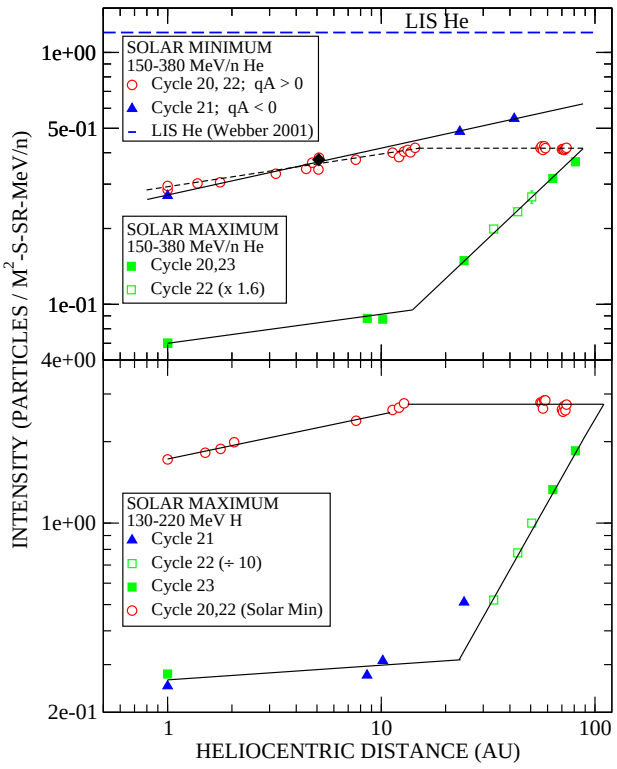

FIGURE 15. Particle intensities: Note that the 130-220 MeV H in 1998 is corrected for ACR H (24±5%). The local interstellar (LIS) H intensity is 23 $m^{-2}s^{-1}sr^{-1}MeV^{-1}$.

variation of the particle diffusion coefficients from the sun to the heliopause.

The Voyagers and Pioneers sample a different region of space over each phase of the solar and heliomagnetic cycles, so we must combine the data to obtain a unified description of the spatial variations at a particular solar cycle phase. The solar minima of cycles 20 and 22 are very similar; Climax neutron monitor counting rates and the IMP 8 H and He spectra were essentially the same in each cycle. Thus the Pioneer and Voyager intensities for these periods can be combined. The radial distribution for the three solar minimum periods for 175 MeV GCR H and 265 MeV/nuc He shows essentially no change in their intensities between about 12 and 73 AU (Figure 15). The latitudinal gradients are small (0.0±0.1%/° for 175 GCR H and 0.0±0.2%/° for 265 MeV/nuc GCR He at 61 AU in 1996). The intensity for these two A>0 periods is 0.295 at 1 AU, 0.43 at 14 AU and 0.44 $m^{-2}s^{-1}sr^{-1}MeV^{-1}$/nuc at 75 AU. The expected value of the interstellar intensity is 1.2 [*Webber and Lockwood*, 2001]. Based on this interstellar intensity and neglecting drift effects, 85% of the GCR He cosmic ray modulation at solar minimum occurs at the TS and in the heliosheath and only 15% occurs inside the TS. Most of this 15% occurs between 1 and 15 AU.

Conventional 2D simulations of the cosmic ray radial distribution at solar minimum show that the effect of increasing the difference between the 1 AU and LIS intensities and reducing g_r to a very small value in the distant heliosphere would be to greatly increase the amount of modulation in the heliosheath for A>0 [*Jokipii et al.*, 1993]. For 175 MeV GCR H with a rigidity of 0.6 GV, drift effects should be smaller, but the radial dependence is very similar to that of GCR He. With an interstellar intensity of 23 $m^{-2}s^{-1}sr^{-1}MeV^{-1}$ and neglecting drifts, <10% of the modulation occurs inside the TS.

5.1 Solar Maximum

At 1 AU the solar maximum intensities are virtually identical for cycles 21 and 23, suggesting that at this time modulation conditions throughout the heliosphere were very similar. Normalizing the 1 AU cycle 22 solar maximum intensity to that of cycles 21 and 23 unifies the solar maximum intensities in a remarkable way. The data in Figure 15 show that the spatial variation of GCR He has the functional form $g_r = J^{-1}dJ/dr = G_0/r$ (where r is the heliocentric distance in AU) with g_r having a value of $10/r$% /AU from 1-15 AU and $g_r = 73/r$% /AU for r> 15 AU.

This procedure can also be applied to 130 - 220 MeV GCR H using a normalizing factor of 1.5 which is very close to the value required for GCR He (Figure 15). The organization of the hydrogen data closely resembles that of GCR He with $g_r = 139/r$ % /AU in the outer heliosphere (Figure 15). The GCR He (1.5 GV), GCR H (0.6 GV), and electrons (0.1 GV) (see Section 2.4) suggest that the heliosheath modulation is strongly rigidity dependent [*Webber and Lockwood*, 2001].

The GCR radial intensity distributions at solar maximum indicate that the changes that produce the 11-year modulation cycle mainly occur in the outer heliosphere between 15 AU and the TS. The extrapolation of the solar maximum data intersects the solar minimum intensity levels at 98.5 AU (GCR He) and 101.5 AU (GCR H). These data suggest that in cycle 23 the heliosheath modulation did not change significantly between 1997-98 and solar maximum in 2001.

5.2 Local Reacceleration of GCR at the TS

The measured intensities in the ecliptic plane of the GCR He (265 MeV/nuc) and ACR oxygen (7-18 MeV/nuc) at 70 AU during the 1996-1998 solar minimum are significantly less than those observed at 42

AU during the 1987 solar minimum. The GCR He at 42 AU is 30% greater than that at 70 AU while the ACR O^+ is five times greater. At 1 AU, the intensities of these two components at these two solar minima differ by only a few percent. The different intensity levels in the opposite phases of the heliomagnetic cycle must be a drift related effect. *Jokipii et. al.* [1993] modeled the transport of GCRs and ACRs in a 2D heliosphere that includes not only drifts but also the effects of an extended heliosheath region. They find that near the plane of the ecliptic in A<0 cycles a significant enhancement of GCRs is produced by local reacceleration in the heliosheath (Figure 15). The model also predicts a much larger increase in the ACR O^+ intensity, consistent with the Pioneer and Voyager observations.

5.3 Mean free paths

We have used the V1 and V2 CRS observations of ACRs to determine the evolution of the radial mean free path from 0.4 GV to 4 GV over the course of the solar cycle beginning in 1990 [*Cummings and Stone* 2001a]. At solar maximum, the mean free path of 1.5 GV particles increases approximately linearly with radial distance, in accordance with expectations from at least one theory [*Bieber and Matthaeus*, 1997]. In addition, the effective radial mean free pathlength is much larger at solar minimum than at solar maximum.

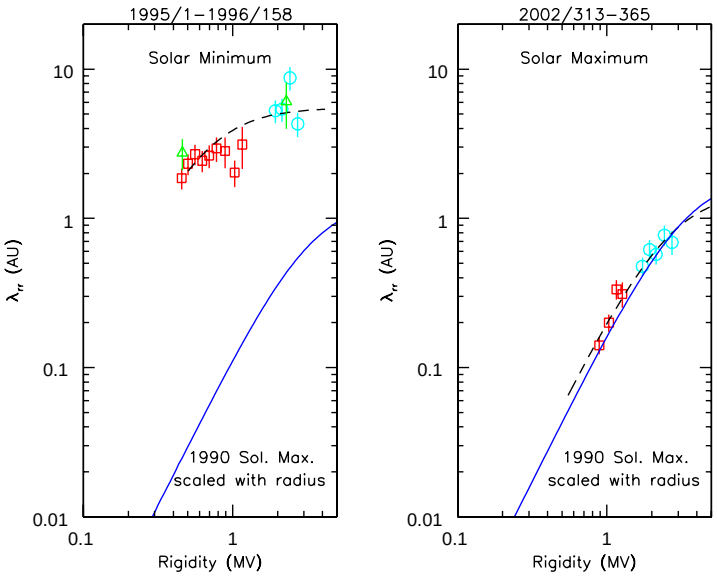

FIGURE 16. Rigidity dependence of the mean free path with distance at solar minimum and solar maximum.

The difference in the rigidity dependence of the mean free path between solar minimum and solar maximum is illustrated in Figure 16. For the solar minimum period, two methods were used to estimate the mean free path: 1) the force field method using the observations of the radial gradient and of the shape of the energy spectra of ACR He and O and 2) anisotropy measurements at V1 of ACR He and O coupled with radial gradient observations. Each panel also shows the rigidity dependence during the 1990 solar maximum [*Stone and Cummings*, 1999] scaled linearly with radius. In the solar minimum period, the mean free paths are much larger than at solar maximum, exceeding the solar maximum value by a factor of 40 at 1 GV. The right panel of Figure 16 shows that for a recent 52-day interval the rigidity dependence of the mean free path is nearly the same as that observed in 1990.

The period of study has included two solar maxima and the intervening A>0 solar minimum period. During the A>0 portion of the 22 year solar cycle, positive particles drift down from higher latitudes towards the heliographic equator. Thus the large mean free paths that we infer may be both a latitude and solar cycle effect. At high latitudes at solar minimum, the solar wind speeds are uniformly high and stream-driven turbulence is weak, so the mean free path is large [*Zank et al.*, 1998]. Near the helioequator, within the streamer belt, more turbulence is present and the mean free paths are shorter. So even though V2 may have been in the streamer belt during the solar minimum observations, the downward drift brought particles from higher latitudes which resulted in small radial gradients and larger effective mean free paths. During solar maximum, enhanced stream-driven turbulence at higher latitudes results in shorter mean free paths and larger radial gradients at all latitudes. The onset of the A<0 solar cycle offers a unique opportunity to determine the evolution of the rigidity and radial dependence of the effective radial mean free path at greater radial distances and higher latitudes.

5.4 GRADIENTS

The last reversal of the Sun's magnetic field occurred at the Sun during 1999-2000. The magnetic topology of the reversal was convected out by the solar wind and reached the vicinity of V1 and V2 during 2000-2001 [*Cummings and Stone*, 2001b], marking the onset of the A<0 portion of the solar cycle in the outer heliosphere when the Sun's magnetic field is inward in the northern hemisphere. The polarity for the prior 10 years was A>0, during which the large-scale curvature and gradient drifts transported positive particles from the polar regions towards the heliographic equator. This flow resulted in positive latitudinal gradients of ACRs and GCRs [*Cummings et al.*, 1995b]. When A<0, the drift directions are reversed and the particles gain entrance into the heliosphere via rapid drift along

the heliospheric neutral current sheet [*Levy*, 1976], resulting in negative latitudinal gradients.

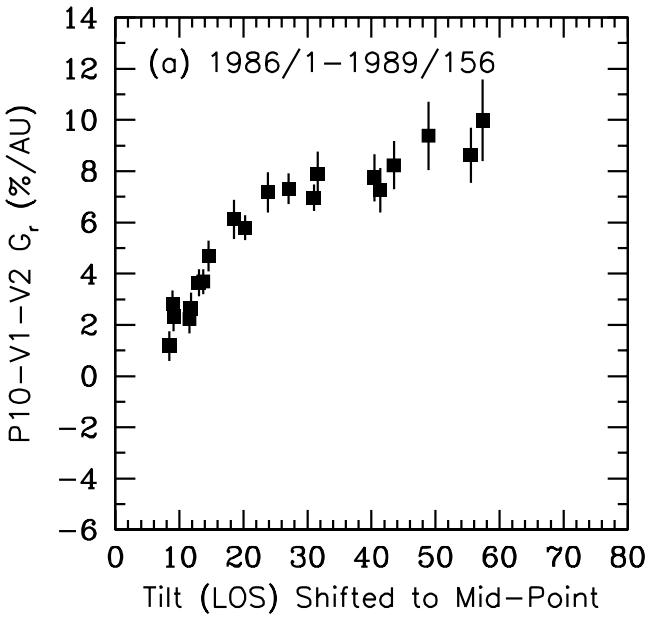

FIGURE 17. Radial gradient vs. inferred tilt of the Current sheet during the last A<0 period in 1986-1989. The figure is adapted from *Stone and Cummings [1999].*

During an A<0 cycle, the radial gradient is correlated with the tilt of the current sheet as shown in Figure 17 for observations near 33 AU in 1986-1989. At 33 AU, drifts along the current sheet appear to determine the radial gradient for tilts up to 30° [see, e.g., *Jokipii et al.*, 1977]. However, for larger tilts when the amplitude of the waviness of the current sheet is >17 AU, the gradient is likely determined by the diffusive radial mean free path. The gradient between V1 and V2 exhibits a similar relationship to the current sheet tilt.

During the current A<0 cycle, the average location of V1 and V2 will be about 86 AU. The transition from a gradient dominated by radial diffusion to one dominated by drifts should occur at a smaller tilt angle because the diffusive radial gradient is expected to be smaller at 86 AU since the mean free path increases linearly with radius.

5.5 Future work

- Observe the GCR recovery and solar minimum of cycle 23 as the Voyagers approach the TS.
- Simulate the GCR and ACR modulation.
- Explore ways to unify data from different spacecraft in more data periods.
- Emphasize combined ACR and GCR studies.
- Determine the evolution of the effective mean free paths in the outer heliosphere during an A<0 period and relate that evolution to changes in the turbulence and magnetic topology of the interplanetary medium in the outer heliosphere.
- Observe the gradient between V1 and V2 and the dependence of the gradient on tilt and radius in order to determine the relative roles and radial dependence of drifts and radial diffusion in the outer heliosphere during A<0.

6. SUMMARY

The Voyager spacecraft continue outward on a mission which has both the promise of encountering truly new heliospheric and extraheliospheric features and an exemplary record of current scientific productivity. First-encounters with the termination shock, heliosheath, heliopause, and interstellar medium will be spectacular milestones in the exploration of our Sun's surroundings. These encounters could answer many basic, long-standing questions about the plasma and magnetic properties of the LISM, the nature of the TS and its role in the acceleration of the ACRs, the role of the heliosheath in GCR modulation, the spectra of low energy interstellar GCRs, and the source and location of the heliospheric radio emissions.

These major milestones ahead should be anticipated but not allowed to overshadow the current contributions of the Voyager mission. The Voyagers are making the first observations of the effects of the interstellar neutrals on the solar wind in the outer heliosphere. Some results were predicted, such as the slowing and heating of the solar wind plasma. But even in those cases aspects of the data were neither predicted nor understood. Other observations have been a surprise, such as the intense anisotropic energetic particle fluxes recently observed by V1. Phenomena such as the heliospheric radio emission were discovered by Voyager and have now been observed through three solar cycles, but their physics is still not understood. Exploratory missions such as Voyager provide key tests of our physical theories and also provide observational surprises which often lead to major advances in physical understanding.

The longevity of the Voyagers makes them ideal platforms for studying long-term solar wind variations. Their distance make them ideal for studying the evolution of the solar wind, shocks, and cosmic rays. The interpretation of Voyager data is greatly enhanced by the ability to compare with data from Earth-orbiting spacecraft (IMP 8, Wind, ACE, SAMPEX), Ulysses, and Pioneers 10 and 11. These data make deconvolution of solar cycle, distance, and latitude effects possible. To further this intercomparison of data sets

and to provide opportunity for the community to provide new insight into these observations, we strongly endorse Guest Investigator and theory programs focusing on the outer heliosphere. Theory and multi-spacecraft comparisons are needed to provide the best understanding of the data Voyager provides.

7. REFERENCES

Bieber, J. W., and W. H. Matthaeus, Perpendicular diffusion and drift at intermediate cosmic-Ray energies, Astrophys. J., 485, 655-659, 1997.

Burlaga, L. F., A heliospheric vortex street, J. Geophys. Res., 95, 4333-4336, 1990.

Burlaga, L. F., and N. F. Ness, Radial and latitudinal variations of the magnetic-field strength in the outer heliosphere, J. Geophys. Res., 98, 3539-3549, 1993.

Burlaga, L. F., and J. D. Richardson, North-south flows at 47 AU: A heliospheric vortex street? J. Geophys. Res., 105, 10501-10507, 2000a.

Burlaga, L. F., N. F. Ness, J. D. Richardson, and R. P. Lepping, The Bastille Day shock and merged interaction region at 63 AU: Voyager 2 observations, Solar Physics, 204 (1-2), 399-410, 2001.

Burlaga, L. F., N. F. Ness, Y.-M. Wang, and N. R. Sheeley Jr., Heliospheric magnetic field strength and polarity from 1 to 81 AU during the ascending phase of solar cycle 23, J. Geophys. Res., 107, 1410, 2002a.

Burlaga, L. F., J. D. Richardson, and C. Wang, Speed fluctuations near 60 AU on scales from 1 day to 1 year: Observations and model, J. Geophys. Res., 107, A10, 1328, 10.1029/2002JA009379, 2002c.

Burlaga, L. F., N. F. Ness, and J. D. Richardson, Sectors in the distant heliosphere: Voyager 1 and 2 observations from 1999 - 2002 between 57 and 83 AU, J. Geophys. Res., in press, 2003a.

Burlaga, L. F., C. Wang, J. D. Richardson, and N. F. Ness, Large-scale magnetic field fluctuations and development of the 1999 - 2000 GMIR: 1 to 60 AU, Ap. J., 582 - 549, 1 Part 1, 2003b.

Burlaga, L. F., C. Wang, N. F. Ness, and J. D. Richardson, Evolution of magnetic fields in corotating interaction regions from 1 to 95 AU: Order to chaos, Ap. J., in press, 2003c.

Burlaga, L. F., C. Wang, J. D. Richardson, and N. F. Ness, Evolution of the multi-scale statistical properties of corotating streams from 1 to 95 AU, J. Geophys. Res., in press, 2003d.

Cummings, A. C., and E. C. Stone, Inferring energetic particle mean free paths from observations of anomalous cosmic rays in the outer heliosphere at solar maximum, in Proc. 27th Internat. Cosmic Ray Conf., Vol. 10, 4243-4246, Hamburg, 2001a.

Cummings, A. C., and E. C. Stone, Onset of solar modulation in the outer heliosphere as seen in anomalous cosmic rays, Proc. 27th Internat. Cosmic Ray Conf., Vol. 10, 4251-4254, Hamburg, 2001b.

Cummings, A. C., R. A. Mewaldt, J. B. Blake, J. R. Cummings, M. Fränz, D. Hovestadt, B. Klecker, G. M. Mason, J. E. Mazur, E. C. Stone, von T. T. Rosenvinge, and W. R. Webber, Anomalous cosmic ray oxygen gradients throughout the heliosphere, Geophys. Res. Lett., 22, 341-344, 1995.

Cummings, A. C., Stone, E. C., and Steenberg, C. D., Composition of anomalous cosmic rays and other heliospheric ions, Astrophys. J., 578, 194-210, 2002a.

Cummings, A. C., Stone, E. C., and Steenberg, C. D., Erratum: "Composition of anomalous cosmic rays and other heliospheric ions", Astrophys. J., 581, 1413, 2002b.

Decker, R. B., E. C. Roelof, and S. M. Krimigis, Solar energetic particle propagation in 1997-99: Observations from ACE, Ulysses, and Voyagers 1 and 2, in Acceleration and Transport of Energetic Particles in the Heliosphere, edited by R. A. Mewaldt, T. H. Zurbuchen, and A. C. Cummings, AIP Conf. Proc. 528, 165, 2000.

Decker, R. B., C. Paranicas, S. M. Krimigis, K. Paularena, and J. D. Richardson, Recurrent ion events and plasma disturbances at Voyager 2 in 5-50 AU, in The Outer Heliosphere: The Next Frontiers, COSPAR Colloquia, edited by K. Scherer, H. Fichtner, H.-J. Fahr, and E. Marsch, Pergamon, New York, 11, 321, 2001.

Decker, R. B., and S. M. Krimigis, Voyager observations of low-energy ions during solar cycle 23, Adv. Space Res., in press, 2003.

Desai, M. I., Mason, G. M., Dwyer, J. R., Mazur, J. E., Gold, R. E., Krimigis, S. M., Skoug, R. M., and Smith, C. W., Evidence for a suprathermal seed population of heavy Ions accelerated by interplanetary shocks near 1 AU, Astrophys. J., in press, 2003

Fichtner, H., Anomalous cosmic rays: Messengers from the outer heliosphere, Space Sci. Rev., 95, 639-754, 2001.

Fisk, L. A., Kozlovsky, B., and Ramaty, R., An interpretation of the observed oxygen and nitrogen enhancements in low-energy cosmic rays, Astrophys. J., 190, L35, 1974.

Gloeckler, G., Observations of injection and pre-acceleration processes in the slow solar wind, Space Sci. Rev., 89, 91-104, 1999.

Goldstein, M. L., D. A. Roberts, L. F. Burlaga, E. Siregar, and A. E. Deane, North-south flows observed in the outer heliosphere at solar minimum: Vortex streets or corotating interaction regions? J. Geophys. Res., 106, 15973-15984, 2001.

Gurnett, D. A., E. Grun, D. Gallagher, W. S. Kurth, and F. L. Scarf, Micron-sized particles detected

near Saturn by the Voyager plasma wave instruments, Icarus, 53, 236-254, 1983.

Gurnett, D. A., W. S. Kurth, F. L. Scarf, J. A. Burns, J. N. Cuzzi, and E. Grun, Micron-sized particles detected near Uranus by the Voyager 2 plasma wave instrument, J. Geophys. Res., 92, 14,959-14,968, 1987.

Gurnett, D. A., W. S. Kurth, L. J. Granroth, S. C. Allendorf, and R. L. Poynter, Micron-sized particles detected near Neptune by the Voyager 2 plasma wave instrument, J. Geophys. Res., 96, 19,177-19,187, 1991.

Gurnett, D. A., Gurnett, J. A. Ansher, W. S. Kurth, and L. J. Granroth, Micron-sized dust particles detected in the outer solar system by the Voyager 1 and 2 plasma wave instruments, Geophys. Res. Lett., 24, 3125-3128, 1997.

Jokipii, J. R., Particle acceleration at a termination shock 1. Application to the solar wind and the anomalous component, J. Geophys. Res., 91, 2929-2932, 1986.

Jokipii, J. R., E. H. Levy, and W. B. Hubbard, Effects of particle drift on cosmic-Ray transport. I. General properties, application to solar modulation, Astrophys. J., 213, 861-868, 1977.

Jokipii, J. R., J. Kota and E. Merenyi, The gradient of galactic cosmic rays at the solar wind termination shock, J. Astrophys. 405, 782, 1993.

Kane, M., R. B. Decker, B. H. Mauk, and S. M. Krimigis, The solar wind velocity determined from Voyager 1 and 2: Low Energy Charged Particle measurements in the outer heliosphere, J. Geophys. Res., 108, 267, 1998.

Kurth, W. S. and Gurnett, D. A., Plasma waves as indicators of the termination shock, J. Geophys. Res., 98, 15,129-15,136, 1993.

Kurth, W. S., and D. A. Gurnett, On the source location of low-frequency heliospheric radio emissions, J. Geophys. Res., in press, 2003.

Langner, U. W., O. C. de Jager, M. S. Potgieter, On the local interstellar spectrum for cosmic ray electrons, Adv. Space Res., 27, 517-522, 2001.

Lazarus, A. J., B. Yedidia, L. Villanueva, R. L. McNutt, Jr., and J. W. Belcher, Meridional plasma flow in the outer heliosphere, Geophys. Res. Lett., 15, 1519-1522, 1988.

Lazarus, A. J., J. D. Richardson, R. B. Decker, and F. B. McDonald, Voyager 2 observations of corotating interaction regions (CIRs) in the outer heliosphere, Space. Sci. Rev., 89, 53-59, 1999.

Le Roux, J. A., Fichtner, H., Zank, G. P., and Ptuskin, V. S., Self-consistent injection and acceleration of Pickup Ions at the solar wind termination shock, Geophys. Res. Lett., 27, 2873-2876, 2000.

Levy, E. H., Theory of the Solar Magnetic Cycle Wave in the Diurnal Variation of Energetic Cosmic Rays: Physical Basis of the Anisotropy, J. Geophys. Res. 81, 2082-2088, 1976.

Liewer, P. C., Goldstein, B. E., and Omidi, N., Hybrid simulations of the effects of interstellar pickup hydrogen on the solar wind termination shock, J. Geophys. Res., 98, 15,211-15,220, 1993.

Liewer, P. C., Rath, S., and Goldstein, B. E., Hybrid simulations of interstellar pickup ion acceleration at the solar wind termination shock, J. Geophys. Res., 100, 19,809-19,818, 1995.

Linde, T. J., Gombosi, T. I., Roe, P. L., Powell, K. G., and DeZeeuw, D. L., Heliosphere in the magnetized local interstellar medium: Results of a three-dimensional MHD simulation, J. Geophys. Res., 103, 1889-1904, 1998.

Macek, W. M., Cairns, I. H., Kurth, W. S., and Gurnett, D. A., Plasma wave generation near the inner heliospheric shock, Geophys. Res. Lett., 18, 357-360, 1993.

McComas, D. J., J. T. Gosling, and R. M. Skoug, Ulysses observations of the irregularly structured mid-latitude solar wind during the approach to solar maximum, Geophys. Res. Lett., 27, 2487-2490, 2000.

McDonald, F. B., B. Klecker, R. E. McGuire, and D. V. Reames, Relative recovery of galactic and anomalous cosmic rays at 1 AU: Further evidence for modulation in the heliosheath, J. Geophys. Res., 107, A8, 2001JA00020, 2002.

McNutt, R. L., Jr., A solar-wind "trigger" for the outer heliosphere radio emissions and the distance to the terminal shock, Geophys. Res. Lett., 15, 1307-1310, 1988.

Mellott, M. M., Subcritical Collisionless Shock Structure, in Collisionless Shocks in the Heliosphere: Reviews of Current Research, edited by B. T. Tsurutani and R. G. Stone, Geophysical Monograph 35, 141-152, 1985.

Ness, N. F., and L. F. Burlaga, Spacecraft studies of the interplanetary magnetic field, J. Geophys. Res., 106 (A8), 15803-15817, 2001.

Opher, M., P. Liewer, T. Gombosi, W. Manchester, D. L. DeZeeuw, K. Powell, I. Sokolov, G. Toth, and M. Velli, 3D MHD description of the region beyond the termination shock: The behaviour of the current sheet, Eos Trans. AGU, 83(47), Fall Meet. Suppl., Abstract SH21A-0485, 2002.

Parker, E. N., Dynamics of the interplanetary gas and magnetic fields, Ap. J., 128, 664, 1958.

Paularena, K. I., C. Wang, R. von Steiger, and B. Heber, An ICME observed by Voyager 2 at 58 AU and by Ulysses at 5 AU, Geophys. Res. Lett., 28, 2755-2758, 2001.

Pesses, M. E., J. R. Jokipii, and D. Eichler, Cosmic ray drift, shock acceleration, and the anomalous component of cosmic rays, Astrophys. J., 246, L85, 1981.

Potgieter, M. S, and Ferreira, S. E. S., Effects of the solar wind termination shock on the modulation of Jovian and galactic electrons in the heliosphere, J. Geophys. Res., 107, A7, 10.1029/2001JA009040, 2002.

Quest, K. B., Simulations of high-mach-number collisionless perpendicular shocks in Astrophysical Plasmas, Phys. Res. Lett., 54, 1872, 1985.

Quest, K. B., Simulations of high Mach number collisionless perpendicular shocks with resistive electrons, J. Geophys. Res., 91, 8805, 1986.

Richardson, J. D., The magnetosheaths of the outer planets, Plan. Sp. Sci, 50, 503-517, 2002.

Richardson, J. D., and K. I. Paularena, Streamer belt structure at solar minima, Geophys. Res. Lett., 24, 1435-1438, 1997.

Richardson, J. D., and C. W. Smith, The radial temperature profile of the solar wind, Geophys. Res. Lett., in press, 2003.

Richardson, J. D., K. I. Paularena, C. Wang, and L. F. Burlaga. The life of a CME and the development of a MIR: From the Sun to 58 AU, J. Geophys. Res., 106, 10.1029/2001JA000175, 2002.

Schwadron, N. A., Combi, M., Huebner, W., and McComas, D. J., The Outer Source of Pickup Ions and Anomalous Cosmic Rays, submitted to Journal of Geophysical Research, 2003.

Slavin, J. D. and Frisch, P. C., The Ionization of Nearby Interstellar Gas, Astrophys. J., 565, 364-379, 2002.

Smith, C. W., Goldstein, M. L., and Wong, H. K., Whistler Wave Bursts Upstream of the Uranian Bow Shock, J. Geophys. Res., 94, 17035-17048, 1989.

Smith, C. W., W. H. Matthaeus, G. P. Zank, N. F. Ness, S. Oughton, and J. D. Richardson, Heating of the low-latitude solar wind by dissipation of turbulent magnetic fluctuations, J. Geophys. Res., 106, 8253-8272, 2001a.

Stone, E. C., News from the Edge of Interstellar Space, Science, 293, 55-56, 2001.

Stone, E. C., and A. C. Cummings, A tilt model for anomalous cosmic rays and the location of the solar wind termination shock, in Proc. 26th Internat. Cosmic Ray Conf., Vol. 7, 500-503, Salt Lake City, 1999.

Strong, A. W., I. V. Moskalenko, and O. Reimer, Diffuse continuum gamma rays from the galaxy, Astrophy. J., 537, 763-784, 2000.

Szabo, A., R. P. Lepping, J. Merka, C. W. Smith, and R. M. Skoug, The evolution of interplanetary shocks driven by magnetic clouds, in Proceedings of "Solar Encounter: The First Solar Orbiter Workshop", pp. 383-387, eds. E. Marsch, V. Martinez Pillet, B. Fleck and R. Marsden, ESA SP-493, Puerto de la Cruz, Tenerife, Spain, 2001.

Wang, C., and J. D. Richardson. Development of a strong shock in the outer heliosphere, Geophys. Res. Lett., 29, 10.1029/2001GL014472, 2002.

Wang, C., and J. D. Richardson, Determination of the solar wind slowdown near solar maximum, J. Geophys. Res., 108, A2, 1058, 10.1029/2002JA009322, 2003.

Wang, C., J. D. Richardson, and J. T. Gosling, A numerical study of the evolution of the solar wind from Ulysses to Voyager 2, J. Geophys. Res., 105, 2337-2344, 2000.

Wang, C., J. D. Richardson, and L. F. Burlaga, Propagation of the Bastille Day 2000 CME shock in the outer heliosphere, Solar Physics, 204 (1-2), 411-421, 2001a.

Wang, C., J. D. Richardson, and K. I. Paularena, Predicted Voyager observations of the Bastille Day 2000 coronal mass ejection, J. Geophys. Res., 106, 13,007-13,013, 2001b.

Webber, W. R., and J. A. Lockwood, Voyager and Pioneer spacecraft measurements of cosmic ray intensities in the outer heliosphere: Toward a new paradigm for understanding the global modulation process, 2, Minimum solar modulation (1987 and 1997), J. Geophys. Res., 106, 29,323-29,332, 2001.

Whang, Y. C., L. F. Burlaga, N. F. Ness, and C. W. Smith, The Bastille Day shocks and merged interaction region, Solar Physics, 204 (1-2), 255-265, 2001.

Zank, G. P., Pauls, H. L., and Williams, L. L., Modeling the Heliosphere, in Proc. Solar Wind, 8, 599-603, 1996a.

Zank, G. P., Pauls, H. L., Cairns, I. H., and Webb, G. M., Interstellar pickup ions and quasiperpendicular shocks: Implications for the termination shock and interplanetary shocks, J. Geophys. Res., 101, 457-477, 1996b.

Zank, G. P., W. H. Matthaeus, J. W. Bieber, and H. Moraal, The radial and latitudinal dependence of the cosmic ray diffusion tensor in the heliosphere. J. Geophys. Res., 103, 20 85-2097, 1998.

Zank, G. P., Interaction of the solar wind with the local interstellar medium: A theoretical perspective, Space Sci. Rev., 89, 413, 1999.

Zank, G. P., W. K. M. Rice, I. H. Cairns, J. W. Bieber, R. M. Skoug, and C. W. Smith, Predicted timing for the turn-on of radiation in the outer heliosphere due to the Bastille Day shock, J. Geophys. Res., 106, 29363-29372, 2001.

Zank, G. P., and H.-R. Mueller, The dynamical heliosphere, J. Geophys. Res., in press, 2003.